ISSN 2282-6483

Alma Mater Studiorum - Università di Bologna
DEPARTMENT OF ECONOMICS

Species Origin and Ecological Context Shape Climate Vulnerability of Temperate Conifers

Maria Elena Bontempi
Clémentine Ols

Quaderni - Working Paper DSE N° 1229

Species Origin and Ecological Context Shape Climate Vulnerability of Temperate Conifers

Maria Elena Bontempi* Clémentine Ols†

July 20, 2026

Abstract

Temperate conifer forests underpin European ecosystems and economies, making it essential to understand how they respond to climate change. Yet most empirical studies estimate average climate responses that mask variability across biological and ecological scales. Using a cross-classified panel model, we estimate heterogeneous climate sensitivities across trees, species, and ecological regions while accounting for temporal dynamics, competition, stand characteristics, and within- and between-species size variation. Spring temperature emerges as the dominant seasonal driver of radial growth, but its effect varies markedly across species and ecological regions. Native species exhibit lower growth potential but more context-dependent responses, whereas introduced species generally achieve higher growth while displaying greater climate sensitivity. Controlling for tree size attenuates the estimated temperature effect, showing that part of the apparent climate response reflects ontogenetic structure rather than intrinsic physiological sensitivity. Consequently, vulnerability cannot be inferred from species identity alone but depends on the interaction between species traits and ecological context. Models imposing homogeneous climate responses therefore risk misrepresenting both resilience and exposure to climate change. Our findings suggest that continued warming and changing precipitation regimes are likely to reshape temperate conifer forests through differential responses across species and ecological settings rather than through a uniform climatic effect.

Keywords: Conifer forests; Climate change; Heterogeneity; Mixed model; Cross-classified panel; Radial increment; Diameter.

JEL classification: Q54, Q23, C23, Q24.

*Department of Economics, University of Bologna, mariaelena.bontempi@unibo.it.

†Service de l'Information Forestière, Institut National de l'Information Géographique et Forestière, Nogent-sur-Vernisson, clementine.ols@ign.fr

Non-technical Summary

Climate change is altering the growth of forests worldwide, but tree species do not all respond in the same way. Even within the same species, trees growing under different environmental conditions may react differently to rising temperatures. Understanding this heterogeneity is essential for predicting future forest productivity and designing effective management strategies.

This study investigates the growth responses of eight conifer species across France using observations from the French National Forest Inventory. Unlike most previous studies, which estimate average climate effects for individual species or regions separately, we analyse species, ecological regions, and individual trees simultaneously within a unified statistical framework. This allows us to distinguish differences due to biological characteristics from those arising from environmental conditions and stand structure.

Our results show that spring climate is the main driver of annual tree growth, but its effects vary considerably across both species and ecological regions. Accounting for differences in tree size explains part of this variation, revealing that some apparent differences in climate sensitivity are actually related to forest structure rather than to intrinsic biological responses. Nevertheless, substantial heterogeneity remains after controlling for these structural factors.

The analysis also highlights systematic differences between native and introduced species. Introduced species generally display higher growth rates, whereas native species exhibit slower but more context-dependent responses. This pattern may reflect different long-term adaptive strategies, with native species potentially adopting more conservative use of water and nutrients under changing environmental conditions.

These findings have important implications for both ecological forecasting and forest management. Models based on average responses may overlook important local differences and produce misleading projections of future forest productivity. More reliable assessments require recognising that climate sensitivity is shaped jointly by species characteristics, ecological context, and forest structure. Promoting structurally diverse forests and species adapted to local conditions is therefore likely to enhance resilience under future climate change.

More broadly, the paper illustrates how statistical methods originally developed in the social sciences can help address complex ecological questions by explicitly modelling multiple sources of heterogeneity.

1 Introduction

Climate change is altering conifer growth dynamics across temperate regions. Rising temperatures, shifting precipitation regimes, and more frequent extremes modify tree growth, species competition, and forest resilience.

Understanding how climate affects forest productivity and stability is central to both ecological sustainability and timber supply. Coniferous forests underpin large segments of the European timber industry and provide essential ecosystem services, including carbon sequestration and watershed protection. As climatic conditions continue to change, identifying which species and ecological contexts are most vulnerable has become a pressing research and management priority.

Most empirical studies estimate climate–growth relationships using average sensitivities for specific species or sites. Such approaches implicitly assume homogeneous climate responses within species or regions. Yet forest ecosystems are inherently heterogeneous systems in which growth reflects species-specific traits, competitive pressure, stand structure, and site conditions, all interacting with climate in complex ways. Ignoring this cross-scale structure may underestimate variability and misrepresent both vulnerability and resilience.

We challenge the homogeneity assumption by modelling heterogeneous climate responses of temperate conifers using a cross-classified multilevel framework. Climate–growth panels are inherently cross-classified: trees are simultaneously embedded within species and ecological regions that intersect but are not hierarchically nested. Rather than absorbing this heterogeneity, we model it explicitly through random intercepts and random climate slopes at species and ecological-region levels. This allows climate sensitivities to vary systematically across biological identity and ecological context, and enables quantification of the extent to which aggregation masks climate vulnerability.

We use data from the French National Forest Inventory (2006–2016), encompassing multiple conifer species, management regimes (native versus afforested), and diverse climatic contexts ranging from oceanic and continental to Mediterranean and mountain environments.

We find pronounced and systematic heterogeneity in climate responses. Spring temperature emerges as the dominant seasonal driver of growth, but its impact varies sharply across species and regions. Native species, although slower growing on average, exhibit greater resistance to heat stress and competition, whereas introduced species display higher baseline growth but greater climate sensitivity.

Ecological context further mediates these patterns, indicating that resilience cannot be inferred from species identity alone. Models based on average sensitivities substantially underestimate this variability.

These findings have implications for forest management under climate change. While pure and even-aged conifer stands have long been favoured for timber efficiency, structurally homogeneous plantations may be more vulnerable to climatic stress. Explicitly accounting for cross-scale heterogeneity provides a more accurate assessment of climate risk and supports adaptive management strategies aimed at enhancing forest resilience.

The remainder of the paper proceeds as follows. Section 2 sketches the ecological and methodological literature on climate–growth analysis. Section 3 describes the data and variables. Section 4 presents the cross-classified modelling framework. Section 5 reports results, including random-slope analyses. Section 6 concludes. Robustness and additional checks are presented in Appendix A.1.

2 Related literature

Conifers dominate much of the forest cover in Central and Northern Europe and constitute the backbone of the European timber industry. Beyond timber production, temperate conifer forests provide a wide range of ecosystem functions and services, including carbon sequestration (Sheikh et al., 2021), groundwater regulation and slope stabilization (Bruijnzeel, 2004), cultural benefits through forest bathing (Shinrin-yoku; Tsunetsugu et al., 2009), and key ecosystem functions such as soil formation, nutrient cycling, and habitat provision (Augusto, De Schrijver, et al., 2015). They also support the production of valuable non-wood forest products, including mushrooms, truffles, resins, and essential oils (Collado et al., 2018). Maintaining these ecological and economic functions ultimately depends on forest growth and productivity, making it essential to understand how conifer growth responds to changing climatic conditions.

Climatic conditions in Europe are changing rapidly, with rising mean annual temperatures, altered precipitation regimes, and increasingly frequent extremes such as heatwaves, storms, and droughts (Intergovernmental Panel on Climate Change, 2022; European Environment Agency, 2020). These climatic shifts are placing European coniferous forests under growing stress (Lindner et al., 2010). In recent decades, widespread crises due to climate change have already occurred. For example, the presence of Norway spruce and Silver fir is seen to be compromised

in favour of broadleaf species, such as European beech (*Fagus sylvatica*). Beech is actually threatened in most continental areas (Lorraine, Black Forest, etc.) due to warming. This is raising concerns about the long-term viability of softwood supply (Allen et al., 2010; Hlásny et al., 2019) and is compromising ecosystem services (Pretzsch et al., 2014; Pan et al., 2011; Hanewinkel et al., 2013; Nabuurs, 2018).

Although timber production has traditionally favoured even-aged, monospecific plantations because of their operational simplicity and high productivity,[1], some foresters are shifting their management paradigm from monocultures of uniform age towards uneven-aged, compositionally diverse forests that rely more heavily on natural regeneration (Brang et al., 2014; Bauhus et al., 2017). This transition is supported by growing evidence that structural and compositional diversity enhances forest resilience and biodiversity (Bremer and Farley, 2010; Liu et al., 2018), increases soil organic carbon storage (Waring et al., 2020; Gong et al., 2025), improves the provision of ecosystem services (Felton et al., 2016), and promotes more efficient resource use through complementarity among age classes (Aakala et al., 2013; Mohr et al., 2024).

The ability of conifers to cope with intensifying climate stress is extremely important but uncertain and difficult to assess. The need to closely monitor interactions between climate and growth and to adapt management strategies accordingly conflicts with the problems encountered in empirical analysis.

Assessing climate impacts on forest usually is based on average sensitivities in specific locations and for specific species: the Silver fir in Basilicata (Gentilesca and Todaro, 2008), the pure Pinus ponderosa of Monument Canyon Research Natural Area in the Jemez Mountains of north-central New Mexico (Evans et al., 2017) and the Douglas fir in western North America (Klesse et al., 2020) are some examples.

Regarding methodology, one stream of studies has applied dendrochronological statistical techniques, based on correlations between filtered growth and climate variables (Gentilesca and Todaro, 2008; Ols, Hervé, et al., 2020; Ols, Gschwantner, et al., 2022). Another line of research has applied regression methods that explicitly incorporate non-climatic drivers of growth (Anderson-Teixeira et al., 2022). Evans et al. (2017), Bauman et al. (2022), and Klesse et al. (2020) exploit hierarchical model to account for trees nested into specific sites.

Unlike previous empirical studies, which typically focus on individual species,

[1]Large forestry companies are increasingly experimenting with highly productive monocultures. For example, in the Landes region of south-western France, eucalyptus plantations have been established alongside the traditional maritime pine forests to explore alternative production systems under future climatic conditions (Bouvet et al., 2013).

specific regions, or separate regression models, we analyse climate–growth relationships using a single national-scale dataset covering temperate European forests. Our specification jointly accounts for multiple sources of heterogeneity, including tree-level characteristics (social status, management history, and within- and between-tree size effects), plot-level conditions (competition), and forest-stand abiotic and structural attributes (elevation, structural heterogeneity, stand density, soil water capacity, temporary waterlogging, and soil properties).

Our work builds upon the dataset of Ols, Hervé, et al. (2020) but introduces a cross-classified mixed modelling framework that explicitly accounts for trees simultaneously belonging to combinations of conifer species and ecological regions across the entire French territory. This framework allows climate sensitivity to vary across both biological and ecological dimensions while controlling for a comprehensive set of determinants of tree growth. Unlike previous empirical studies, which typically focus on individual species, specific regions, or estimate simple bivariate regressions, we analyse climate–growth relationships using a large-scale national dataset and a unified modelling framework. Our specification jointly accounts for multiple sources of heterogeneity, including tree-level characteristics (social status, management history, and within- and between-tree size effects), plot-level conditions (competition), forest-stand abiotic and structural attributes (elevation, structural heterogeneity, stand density, soil water capacity, temporary waterlogging, and soil properties), and interactions among climatic variables. This framework enables us to disentangle structural differences in tree growth from genuine differences in climate sensitivity across species and ecological regions.

3 The data

The empirical analysis relies on the dataset from Ols, Hervé, et al. (2020), which is based on 10.643 trees sampled across the systematic grid of the continuous French National Forest Inventory (NFI) over the 2006–2016 period, combined with the European E-OBS gridded climate dataset at a $0.25^{\circ} \times 0.25^{\circ}$ resolution (Cornes et al., 2018). This dataset was specifically selected to investigate the response of Western European conifers to climatic variability in pure and even-aged stands, exploiting bioclimatic ecoregions that partition the French territory and are representative of the coniferous forests distributed across Europe.

The French NFI constitutes one of the most comprehensive forest monitoring systems worldwide. Since 2005 it has adopted an annualized sampling design

based on a 1×1 km grid. Every year one tenth of the grid is inventoried and 7,000 plots, classified as forests by the photo interpretation of aerial images, are visited in the field in order to deliver fully renewed information on forests. Sampling plots are *temporary* and consist in 25-m radius circles within which forest composition and stand structure, ground vegetation, soil conditions, topography (elevation, soil type, etc.) are described and trees measured. Tree cores are also collected on two dominant trees, chosen within the main tree species encountered on the plot, for age estimation and annual radial increment measurement.[2] Each year the sampled plots (and trees) change. The plots inventoried each year cover the entire national territory. Forests cover 31% of the French territory, with different conifers accounting for 21% of this area (see `inventaire-forestier.ign.fr`).

France presents one of the largest European climatic diversity, from the warm and dry Mediterranean south to the cold and humid alpine zones, while intermediate oceanic and continental regions exhibit more moderate conditions. - including oceanic, continental, Mediterranean and alpine conditions. Such environmental heterogeneity makes the country a privileged setting for analysing tree growth under diverse regimes.

This dataset is very interesting as it is not based on a single species in a specific region (unlike most of the analyses produced by the dendroecological literature), thus allowing for exploring the differences in growth induced by climate change in terms of changed temperatures and precipitation regimes. The distribution of species by ecological regions, with identification of whether native or afforested, is in Table 1.

In the Ols, Hervé, et al. (2020) dataset, approximatively 88% of tree-species appear in more than one ecological region, while only 12% (European larch, Aleppo pine, Corsican pine) are completely contained in a single ecological region. Ecological regions have trees up to four different species; only 29.7% of ecological regions have trees from a single species (Semi-continental east, Oceanic south west and Mediterranean). Afforested trees account for 36.16% of the total. Native species, such as European larch, Aleppo pine and Silver fir, occur naturally within French forests, each being dominant in specific ecological zones (Alps, Mediterranean and Vosges, respectively). Other conifers (Douglas fir -originating from North America, Corsican Pine -native to Corsica and Maritime Pine -originally from southern Turkey) are only afforested (in Semi-Oceanic Central North and Massif Central,

[2]Cores are extracted at breast height (approximately 1.30m above ground) perpendicularly to the stem, using an increment borer, mounted directly in the field with a precision of 1/10mm.

Table 1: Distribution of Tree Species by Ecological regions

	1-Crystalline Oceanic West	2-Semi-Oceanic Central North	3-Semi-Continental East	4-Vosges	5-Oceanic South West	6-Massif Central	7-Alps	8-Mediterranean	Total
Douglas fir	0	551 (A)	0	0	0	1,145 (A)	0	0	1,696
		(48.7)				(35.9)			(15.9)
Norway spruce	0	0	337 (A)	303	0	730 (A)	279	0	1,649
			(100)	(47.8)		(22.9)	(19.3)		(15.5)
European larch	0	0	0	0	0	0	341	0	341
							(23.6)		(3.2)
Aleppo pine	0	0	0	0	0	0	0	455	455
								(100)	(4.3)
Corsican pine	482 (A)	0	0	0	0	0	0	0	482
	(44.5)								(4.5)
Maritime pine	602 (A)	0	0	0	2,366 (A)	0	0	0	2,968
	(55.5)				(100)				(27.9)
Scots pine	0	581 (A)	0	0	0	725	826	0	2,132
		(51.3)				(22.7)	(57.1)		(20.0)
Silver fir	0	0	0	331	0	589	0	0	920
				(52.2)		(18.5)			(8.6)
Total	1,084	1,132	337	634	2,366	3,189	1,446	455	10,643
	(10.19)	(10.64)	(3.17)	(5.96)	(22.23)	(29.96)	(13.59)	(4.28)	(100)

Note: (A) for afforested trees. Introduced trees represent the 36.16% of total trees.

Crystalline-Oceanic West, and Crystalline-Oceanic West and Oceanic South West, respectively). Semi-Continental East have only one species of afforested trees, Norway spruce. Norway spruce and Scots pine are species native to France (in Vosges, Alps, and Massif Central) but were also introduced in specific lands (Semi-Continental East, Massif Central). Massif Central has a mixture of native and afforested trees, while most ecological regions, with the exception of the Vosges, the Alps and the Mediterranean, have only afforested trees.

Table 1 can be translated into the map, rearranged from Ols, Hervé, et al. (2020), and the species reported in Figure 1:

The data are unbalanced but this does not prevent us from conducting a multi-level analysis. From Table 1, immediately it emerges that the panel is not a strict three-level hierarchy of trees nested into species and nested into regions. Rather it is a partially crossed ecological classification where trees are nested within the cells formed by the cross-classification of species-by-ecological regions. This implies that there are two separate two-level hierarchies which cross one another: (1) a tree-plot-within-specie hierarchy, and (2) a tree-plot-within-ecological-region hierarchy. Indeed, trees are nested within species but not all trees from the same species live in the same ecological region and, simultaneously, the ecological region identifiers are not constant within each specie unit.

3.1 Metrics of Forest Growth: Diameter vs. Radial Increment

In recent literature, the most common measures for tree growth are diameter and radial increment (tree-ring width), with the latter largely prevailing due to its higher

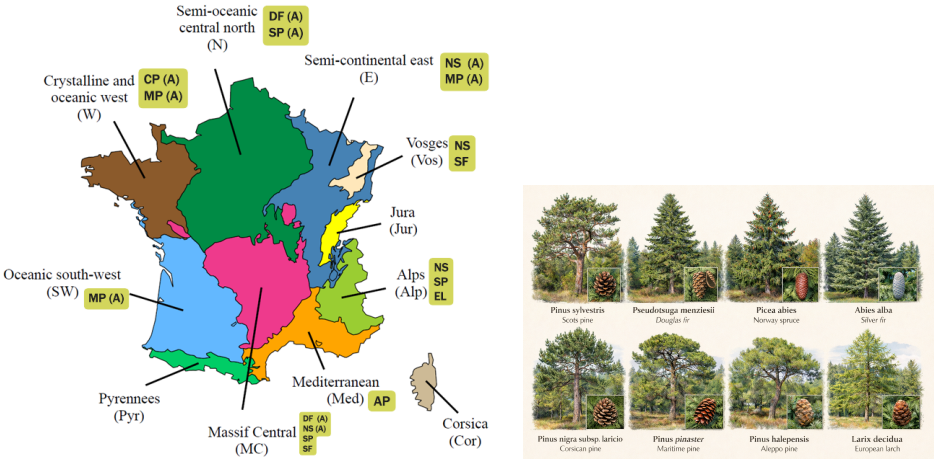

(a) *Distribution of species by ecological regions.* (b) *Species*

Figure 1: Ecological regions and species

Note: (A) stands for afforested. Species abbreviations: DF = Douglas fir, NS = Norway spruce, EL = European larch, AP = Aleppo pine, CP = Corsican pine, MP = Maritime pine, SP = Scots pine, SF = Silver fir.

temporal resolution and sensitivity to environmental variation.

Diameter is widely used in large-scale forest monitoring and inventory studies. It is non-destructive, quick to collect in the field, and scalable to millions of trees, providing a standardized metric that facilitates comparisons across sites and over time. Diameter is therefore an ideal metric for achieving extensive spatial coverage in long-term forest monitoring programs (Magarik et al., 2019), detecting mortality events by comparing successive inventory cycles (Kitikidou and Apostolopoulou, 2011), implementing allometric models to estimate biomass and carbon stock changes (Gschwantner et al., 2016).

Whereas diameter increments are good indicators of long-term forest growth, radial increment—measured as annual tree-ring width—offers much finer temporal resolution and greater sensitivity to short-term environmental fluctuations (Evans et al., 2017).

Hence, to capture annual growth of trees, we use the logarithm of the annual radial increment, $\log(ri1)$, where $ri1$ is the width of the last completed tree ring [m] formed by the sampled trees in each year t. The use of log is almost equivalent to the Box-Cox transformation used by Ols, Hervé, et al. (2020). It stabilises the variance, as heteroskedasticity is usually observed in tree growth data. It deals with skewness, as some trees can grow much more than others. The coefficients are interpretable as percentage changes, hence comparable among diverse species and

ecological regions.

While radial increment is a flow variable, diameter at breast height (DBH, 1.30 meters above the ground) [m] represents a state-level variable, reflecting cumulative growth induced by decades of past temperatures and environmental conditions. We use it as an additional control (robustness check) for the size structure and the possibility that trees with higher baseline growth tend to have lower radial increment, an element that could bias the estimated temperature sensitivity. Indeed, the fastest radial growth, i.e. largest tree-ring width, occurs at intermediate sizes, when trees are able to incorporate nutrients efficiently and are less constrained by hydraulic limitations or biomechanical stress, while, at larger sizes, radial growth declines and trees become more sensitive to climate variability (Anderson-Teixeira et al., 2022; Ryan and Yoder, 1997; Mencuccini et al., 2005).

Plots in Figure 2 illustrate the in-sample substantial heterogeneity in both radial increment and diameter across the observed species-ecoregion combinations for afforested (top) and native (bottom) conifers. Boxes show the interquartile range with medians; whiskers extend to the most extreme observations within 1.5 interquartile ranges, and points denote observations beyond the whiskers; the dashed horizontal lines are the overall averages. Only observed species–ecoregion combinations are displayed. Sample sizes range from 341 (European larch–Alps) to 1,696 (Douglas fir–Massif Central), as reported in Table 1.

Afforested species have systematically higher median radial increment, larger dispersion and more extreme high-growth trees than native species. Native species are generally slower growing with tighter distributions than afforested species, but still substantial variability depending on ecological region. The greatest average radial increment is observed in the introduced species Douglas fir, Maritime pine and Norway spruce. The trees with the largest diameter are the native species Silver fir, Norway spruce and European larch, whereas Norway spruce has a smaller diameter when introduced.

While diameter distributions overlap considerably across several combinations, radial increment exhibits much stronger differentiation, suggesting that current growth differences cannot be explained solely by differences in tree size. Figure 2 motivates the unconditional variance decomposition, the conditional multilevel models, the investigation of climate heterogeneous effects and the explicit control for ontogenetic structure introduced later through the within–between decomposition of diameter that are presented in next Section 4..

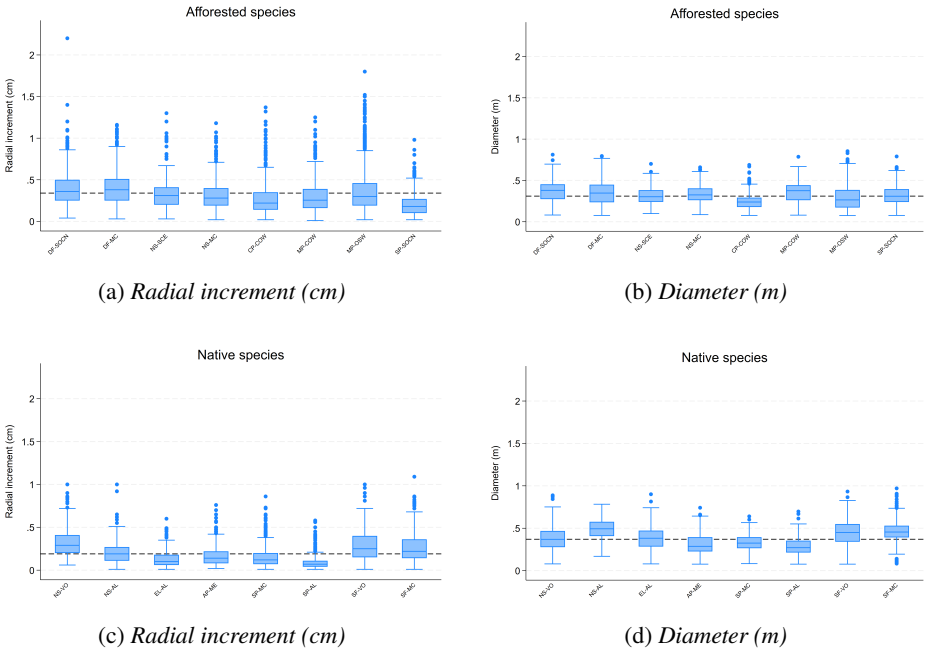

(a) *Radial increment (cm)* (b) *Diameter (m)*

(c) *Radial increment (cm)* (d) *Diameter (m)*

Figure 2: Distribution of radial increment and diameter across observed species and ecological regions combinations

Note: Species abbreviations: DF = Douglas fir, NS = Norway spruce, EL = European larch, AP = Aleppo pine, CP = Corsican pine, MP = Maritime pine, SP = Scots pine, SF = Silver fir. Ecological regions: COW = Crystalline and Oceanic West, SOCN = Semi-oceanic Central North, SCE = Semi-continental East, VO = Vosges, OSW = Oceanic South West, MC = Massif Central, AL = Alps, ME = Mediterranean.

4 Methodology and model

We employ a methodology able to respect the characteristics of the French NFI (temporary sampling plots and trees that change each year), maintain the disaggregated, multilevel structure of the panel and use a multiple regression model to avoid bias from omitted variables. In fact, to understand (and monitor) climate-growth interactions, the methodology must consider that: (1) there are limitations to tree growth induced by competition between trees for nutrients, sunlight and water; (2) climatic conditions vary from region to region, as their effects depend on specific abiotic characteristics of the plot, such as soil types; (3) each species may react differently to climatic conditions (biotic factors).

We implement cross-classified multilevel models, which are better suited to capture the crossed structure of the dataset, where each tree belongs simultaneously to a specie and ecological region. This framework makes it possible to account

for heterogeneity at multiple levels and to obtain a robust understanding of the determinants of tree growth.

We use the notation typical of cross-classified models (Goldstein, 2011; Rasbash and Goldstein, 1994; Rasbash and Browne, 2001; Rasbash and Browne, 2008; Beretvas, 2011) where level-1 observations (tree-plot-year observations) are grouped by two higher-level classifications which are not nested within each other. We set $j_1 = 1, \ldots, J_1$ for species and $j_2 = 1, \ldots, J_2$ for ecological regions, so that the pair (j_1, j_2) indexes the cells of the cross-classification. Within each cell, $i = 1, \ldots, N_{(j_1,j_2)}$ indexes tree-plot units and $t = 1, \ldots, T$ indexes repeated annual observations. The structure is depicted in Figure 3.

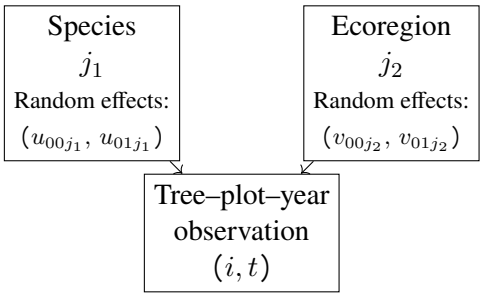

Figure 3: Cross-classified structure: tree–plot–year observations are jointly classified by species and ecological region. Random intercepts, u_{00j_1} and v_{00j_2}, and slopes, u_{01j_1} and v_{01j_2}, are estimated at both higher levels.

The conditional mixed cross-classified model to explain $y_{i(j_1,j_2)t}$, the logarithm of radial increment, is:

$$
\begin{aligned}
y_{i(j_1,j_2)t} &= \beta_{0(j_1,j_2)} + \mathbf{X}'_{i(j_1,j_2)t}\,\boldsymbol{\beta} + \theta_{j_1,j_2}\, z_{pc(j_1,j_2)t} + \varepsilon_{i(j_1,j_2)t}, \qquad (1)\\
\beta_{0(j_1,j_2)} &= \beta_{000} + \beta_{j_1,j_2}\, year_t + u_{00j_1} + u_{00j_2},\\
\theta_{j_1,j_2} &= \theta_{000} + u_{01j_1} + u_{01j_2}
\end{aligned}
$$

In the equation (1) we use compact indexing to keep the model readable. The vector $\mathbf{X}_{i(j_1,j_2)t}$ denotes the stacked vector of all covariates with fixed (group-invariant) coefficients, and $\boldsymbol{\beta}$ is the corresponding conformable parameter vector.

Specifically, we partition $\mathbf{X}_{i(j_1,j_2)t}$ as

$$\mathbf{X}_{i(j_1,j_2)t} = \begin{bmatrix} \mathbf{x}_{i(j_1,j_2)t} \\ \mathbf{x}_{ip(j_1,j_2)t} \\ \mathbf{x}_{p(j_1,j_2)t} \\ \mathbf{x}_{pc(j_1,j_2)t} \end{bmatrix}, \qquad \boldsymbol{\beta} = \begin{bmatrix} \boldsymbol{\beta}_1 \\ \boldsymbol{\beta}_2 \\ \boldsymbol{\beta}_3 \\ \boldsymbol{\beta}_4 \end{bmatrix},$$

Hence, $\mathbf{X}'_{i(j_1,j_2)t}\,\boldsymbol{\beta} = \mathbf{x}'_{i(j_1,j_2)t}\,\boldsymbol{\beta}_1 + \mathbf{x}'_{ip(j_1,j_2)t}\,\boldsymbol{\beta}_2 + \mathbf{x}'_{p(j_1,j_2)t}\,\boldsymbol{\beta}_3 + \mathbf{x}'_{pc(j_1,j_2)t}\,\boldsymbol{\beta}_4$, i.e. it collects tree-level covariates, $\mathbf{x}_{i(j_1,j_2)t}$, tree-plot-level covariates, $\mathbf{x}_{ip(j_1,j_2)t}$, forest stand-level covariates, $\mathbf{x}_{p(j_1,j_2)t}$ and the plot-specific seasonal climate controls, $\mathbf{x}_{pc(j_1,j_2)t}$. The term $z_{pc(j_1,j_2)t}$ includes the climatic covariate whose coefficient is allowed to vary (random slope) by species, j_1, and ecological region, j_2. The group-specific marginal effect θ_{j_1,j_2} equals the grand-mean effect θ_{000} plus the random deviations u_{01j_1} and u_{01j_2}, capturing systematic departures from the overall mean at the species and ecological region levels. The measurement level of each covariate is described in detail below.

The literature does not yet provide sufficiently comparable estimates of heterogeneous climate sensitivity in temperate conifers to support genuinely informative ecological priors. In that situation, Maximum Likelihood is arguably the more scientifically defensible choice able to produce empirical Bayes predictors. Species and ecological regions are each characterized by a random intercept and a random temperature slope. Their covariance allows intrinsically fast-growing groups to differ systematically in climate sensitivity. Hence, species- and ecoregion-level random effects are assumed jointly normally distributed with zero means and unstructured 2×2 covariance matrices:

$$\begin{bmatrix} u_{00j_1} \\ u_{01j_1} \end{bmatrix} \sim \mathcal{N}\left(\begin{bmatrix} 0 \\ 0 \end{bmatrix}, \boldsymbol{\Sigma}_{j_1} \right), \qquad \boldsymbol{\Sigma}_{j_1} = \begin{bmatrix} \sigma^2_{u_{00j_1}} & \sigma_{u_{00j_1},u_{01j_1}} \\ \sigma_{u_{00j_1},u_{01j_1}} & \sigma^2_{u_{01j_1}} \end{bmatrix}$$

$$\begin{bmatrix} u_{00j_2} \\ u_{01j_2} \end{bmatrix} \sim \mathcal{N}\left(\begin{bmatrix} 0 \\ 0 \end{bmatrix}, \boldsymbol{\Sigma}_{j_2} \right), \qquad \boldsymbol{\Sigma}_{j_2} = \begin{bmatrix} \sigma^2_{u_{00j_2}} & \sigma_{u_{00j_2},u_{01j_2}} \\ \sigma_{u_{00j_2},u_{01j_2}} & \sigma^2_{u_{01j_2}} \end{bmatrix}$$

Residuals are assumed normally distributed with a variance which is allowed to differ across species: different conifer species exhibit markedly different intrinsic growth variability, violating homoskedasticity.

$$\varepsilon_{i(j_1,j_2)t} \sim \mathcal{N}\left(0, \sigma^2_{\varepsilon j_1}\right).$$

In the fixed component of the model, we include interactions between the centred calendar year (2006-2016) and each species and ecological region combination. Formally, each group $(j_1 \times j_2)$ is allowed to have its own linear time trend $\beta_{(j_1,j_2)}\, year_t$, which enters the intercept $\beta_{0(j_1,j_2)}$.[3]

These group-specific deterministic trends serve two purposes. First, they capture long-run non-climatic dynamics in growth that may vary systematically across species and regions, such as forest maturation and ageing, nitrogen deposition, recovery from past disturbances, changes in inventory protocols, and management legacies. Because these processes evolve slowly and may not be fully observed, allowing flexible species-region trends reduce omitted-variable bias arising from unobserved structural changes.

Second, climate variables themselves exhibit secular trends. In Europe (European Environment Agency, EEA), spring temperatures have increased markedly over recent decades, with spatially heterogeneous precipitation patterns. Without group-specific time trends, such gradual climate shifts could be confounded with long-run structural growth dynamics, biasing estimates of short-term climate sensitivity. Allowing each species-ecoregion group to follow its own baseline trajectory therefore improves identification of inter-annual growth responses to climate.

We model these trends as fixed effects rather than random slopes because the number of species–region combinations is moderate and the trends are nuisance parameters rather than objects of inference. A random-slope specification for year would impose a distributional structure on deterministic structural change that lacks biological justification and would introduce unnecessary shrinkage.

The climate coefficients are identified from deviations of $\mathbf{x}_{pc(j_1,j_2)t}$ and $z_{pc(j_1,j_2)t}$ from the species–ecoregion-specific linear trend. Because year is centred, the fixed intercept corresponds to mean growth at the sample midpoint. The variance components of the random slopes are identified from cross-group dispersion in estimated group-specific slopes and require sufficient replication across species and regions.

Our model includes various sets of explanatory variables. The tree level variables capture qualitative aspects of individual trees, their social status and management. The combined tree / plot level variables capture competition among trees and

[3]The calendar year variable is centred to reduce collinearity between the trend and the intercept and to facilitate interpretation of the intercept as average growth at the midpoint of the observation period.

the emergence of trees that tower above even the focal tree. The forest stand-level variables measure abiotic conditions (soil chemistry, elevation) and heterogeneity in the stems. Finally, the climate-plot variables capture seasonal precipitations and temperatures and their interactions; these variables include $z_{pc(j_1,j_2)t}$ for which we estimate group-specific (species and region) random slopes.

Tree-level variables, $\mathbf{x}_{i(j_1,j_2)t}$:

- *Social status* (ss). Social status of the targeted tree within the forest stand, defined as the ratio between the tree's diameter and the quadratic mean diameter of the stand. This index captures relative dominance and resource access. Trees are classified as dominant if $ss > 2.5$, co-dominant if $1.5 < ss \leq 2.5$, dominated if $1 < ss \leq 1.5$, and subjected or subjugated if $ss \leq 1$. A positive effect on radial growth is expected, as dominant trees have preferential access to light and soil resources.

- *Native status* ($native$). Indicator variable equal to 1 for native species (time invariant). This distinction reflects differences in ecological adaptation, management history, and potential responses to climatic variability. A negative direct effect on growth is expected, as introduced (afforested) species are often selected for higher productivity.

- *Diameter at breast height* (DBH). Diameter, measured at 1.30 m above ground [m], is used to control for tree size distribution and ontogenetic effects (declining radial increment as trees grow larger).

  To avoid simultaneity between radial increment in year t and diameter measured in the same year, we compute the diameter at the beginning of the growing season that produced the observed ring as $\mathrm{dia}_{i(j_1,j_2)t} = \log\big(DBH_{i(j_1,j_2)t} - 2 \times RI_{i(j_1,j_2)t}\big)$.[4] To disentangle within-tree (ontogenetic) and between-group (size-structure) effects, we apply a within–between (Mundlak-type; Mundlak, 1978) decomposition: Let

$$\overline{\mathrm{dia}}_{j_1,j_2} = \frac{1}{N_{j_1,j_2}} \sum_{i,t} \mathrm{dia}_{i(j_1,j_2)t}$$

  denote the mean log-diameter in species–ecoregion cell (j_1, j_2) computed over the sample period, where N_{j_1,j_2} is the total number of observations in

[4]Because diameter is predetermined relative to the current-year radial increment, it functions as a state variable rather than a simultaneous regressor, reducing concerns about endogeneity in contemporaneous growth estimation.

that cell. The within–between decomposition is defined as

$$\mathrm{dia}_{W,i(j_1,j_2)t} = \mathrm{dia}_{i(j_1,j_2)t} - \overline{\mathrm{dia}}_{(j_1,j_2)}, \quad \mathrm{dia}_{B,(j_1,j_2)} = \overline{\mathrm{dia}}_{(j_1,j_2)} - \overline{\mathrm{dia}},$$

where $\overline{\mathrm{dia}} = (J_1 J_2)^{-1} \sum_{j_1=1}^{J_1} \sum_{j_2=2}^{J_2} \overline{\mathrm{dia}}_{(j_1,j_2)}$ is the grand mean across species-ecoregion cells. The within component $\mathrm{dia}_{W,i(j_1,j_2)t}$ captures ontogenetic deviations within cells, while the between component $\mathrm{dia}_{B,(j_1,j_2)}$ captures persistent differences in mean size across species–ecoregion combinations. Including both terms prevents confounding size-related structural differences with climate sensitivity.

Tree-plot-level variables variables, $\mathbf{x}_{ip(j_1,j_2)t}$:

- *Wolf-tree indicator* ($wolftree$). Formally, let $bal_{i(j_1,j_2)t}$ denote the basal area, [m^2], of trees larger than the focal tree, and let $qmd_{(j_1,j_2)t}$ denote the forest stand variable equal to the quadratic mean diameter, [m^2], of the stand. The indicator is equal to 1 if this basal area over the plot quadratic mean diameter is larger than the basal area of the focal tree in relation to the basal area of the forest stand, [%]. It is a measure of asymmetric competition and we expect a negative effect on radial increment of wolf-trees as they are larger than the focal tree, hence able to dominate light and soil resources.

Forest stand variables, $\mathbf{x}_{p(j_1,j_2)t}$, characterizing abiotic and structural conditions under which trees grow:

- *Elevation* ($alti$). Elevation of the plot above sea level [m]. Elevation captures large-scale climatic gradients (temperature, precipitation, snow cover) and site-specific ecological suitability. The effect may differ across species: for example, Norway spruce, European larch, and Corsican pine are typically better adapted to higher altitudes, particularly in warmer regions.

- *Gini index* ($gini$). Index of stem diameter heterogeneity within the stand, ranging from 0 (perfectly homogeneous) to 1 (maximally heterogeneous). Higher structural inequality may intensify competition for light and soil resources, leading to a negative effect on radial growth. However, heterogeneity may also reflect structural complexity; hence the sign is ultimately empirical.

- *Relative Density Index* (rdi). Reineke's self-thinning index, measuring stand density relative to the theoretical maximum density. Values approaching

or exceeding one indicate overcrowding and strong competition, which is expected to reduce growth.

- *Maximum field water capacity* ($wfcC$). Soil water-holding capacity at 1 m depth [mm]. Higher values indicate greater potential water availability, which should positively affect growth in the absence of waterlogging or harvest disturbances.

- *Water capacity* × *temporary waterlogging* ($wfcC \times tlogC$). Interaction between soil water capacity and the ground-flora-based soil temporary waterlogging index. The latter distinguishes well-drained soils ($tlogC < -0.05$), drained soils ($-0.05 \leq tlogC < 0$), soils with tendency to waterlogging ($0 \leq tlogC < 0.05$), and frequent waterlogging ($tlogC \geq 0.05$). This interaction captures the possibility that high water capacity becomes detrimental when drainage conditions are poor. Controlling for this interaction is essential when evaluating precipitation effects.

- *Carbon-to-nitrogen ratio* (cn_ratio). Ground-flora-based soil C:N ratio. Higher ratios indicate lower nitrogen availability. Since nitrogen is a limiting nutrient for tree growth, a negative effect on radial increment is expected.

- *Base cations* × *subacid soils* ($base\_cation \times phD$). Interaction between $base\_cation$, the soil base cation availability (Ca^{2+}, Mg^{2+}, K^{+}, Na^{+}), and the indicator for subacid soils ($phD = 1$ if $4.5 \leq pH \leq 6$). Conifers generally prefer moderately acidic soils; excessive base saturation can induce root stress. We therefore allow the effect of base cation availability to differ in subacid soils, with high base saturation having a negative effect which is higher in subacid soils.

- *Soil phosphorus* ($p2o5$). Ground-flora-based soil phosphorus content (log-transformed P_2O_5). Phosphorus availability is expected to positively influence radial growth.

Climatic variables, plot-specific seasonal climate conditions, $\mathbf{x}_{pc(j_1,j_2)t}$ and $z_{pc(j_1,j_2)t}$

The climatic covariates $\mathbf{x}_{pc(j_1,j_2)t}$ with fixed parameters include:

- *Spring minimum temperature* ($tmin\_sprC$, [°C]). Included to control for late frost damage and cold limitation of cambial reactivation, particularly in high-elevation or northern sites.

- *Summer precipitation* × *maximum temperature interaction* ($prec\_sumC \times tmax\_sumC$). This term captures heat–drought stress during summer, when high temperatures increase evapotranspiration and respiration losses, especially under Mediterranean or continental climate regimes.

- *Spring precipitation* ($prec\_sprC$, [mm]). Seasonal precipitation sum in spring, capturing soil water availability at the onset of cambial activity.

- *Spring temperature* × *precipitation interaction* ($prec\_sprC \times tmean\_sprC$). This interaction accounts for the joint role of temperature and soil moisture during cambial reactivation. Warmer springs may enhance growth when water is sufficient but amplify stress under dry conditions.

The variable $z_{pc(j_1,j_2)t}$ is *spring mean temperature* ($tmean\_sprC$, [°C]). This variable captures the growth potential induced by photosynthesis and cambial reactivation during the early growing season. Spring temperature is allowed to have a group-specific slope, reflecting the fact that species and ecological regions are separate latent sources of heterogeneity in climate sensitivity. This allows for testing whether climate sensitivity is more taxonomic or ecological. Relative to a specification with a single random slope at the species–ecoregion level, our decomposition operated by the cross-classified model improves statistical efficiency with uneven data through species effects informed by all regions and region effects informed by all species (partial pooling) and enables biologically interpretable inference on the sources of growth–climate variability.

We explicitly test the ecological hypothesis that spring climatic conditions exert a stronger influence on conifer radial growth than summer or other seasonal conditions (see Appendix A.1). The early growing season determines cambial activation, carbohydrate allocation, and the potential for annual increment formation, thereby setting the stage for overall growth performance.

The conditional models we estimate are summarised in Table 2.

The fixed effects model, FE, considers the combinations of species and ecological region as individual heterogeneities that also contribute to the cluster correction of standard errors. The cross-classified mixed model, MM, considers random effects only in the intercept for both species, u_{00j_1}, and the ecological region, u_{00j_2}. The cross-classified mixed model, MMR, adds to the MM model the random slope for temperature at the ecological region level, u_{01j_2}, whereas the cross-classified mixed model, MMS, adds to the MM model the random slope for temperature at

Table 2: Progressive specification of the models.

	FE	MM	MMR	MMS	MMRS	MMRSD
Species × Ecoregion trends	✓	✓	✓	✓	✓	✓
Climate covariates $\mathbf{x}_{pc(j_1,j_2)t}$	✓	✓	✓	✓	✓	✓
Tree-, tree-plot- and forest-stand controls	✓	✓	✓	✓	✓	✓
Species intercept (u_{00j_1})	–	✓	✓	✓	✓	✓
Ecoregion intercept (u_{00j_2})	–	✓	✓	✓	✓	✓
Species slope (u_{01j_1}) for $z_{pc(j_1,j_2)t}$	–	–	–	✓	✓	✓
Ecoregion slope (u_{01j_2}) for $z_{pc(j_1,j_2)t}$	–	–	✓	–	✓	✓
Diameter controls ($ldiam_W, ldiam_B$)	–	–	–	–	–	✓

Note: Model sequence used to assess heterogeneous climate sensitivity. FE absorbs species–ecoregion heterogeneity through combination fixed effects and cluster standard errors. MM introduces crossed random intercepts for species and ecological regions. MMR and MMS add random spring-temperature slopes at the ecological-region and species levels, respectively. MMRS allows both sources of slope heterogeneity. MMRSD further controls for within- and between-group diameter, isolating climate sensitivity conditional on size structure.

the species level, u_{01j_1}. The cross-classified mixed model, MMRS, has random intercepts, u_{00j_1} and u_{00j_2}, and random slopes for temperature at both species and ecological region levels, u_{01j_1} and u_{01j_2}. Finally, the MMRSD model adds diameter, as a robustness check for structural differences in tree size, to the MMRS model.

5 Results

We first quantify how growth variation partitions across species, ecological regions, and individual trees before introducing explanatory variables. This provides an empirical justification for the multilevel cross-classified specification adopted in equation (1). Unconditional models for radial increment are in Table 3.

The unconditional variance decomposition confirms substantial dependence among observations. Growth variability is jointly structured across species, reflecting biological differences, and ecological regions, reflecting environmental and site conditions, making a cross-classified specification preferable to models that ignore clustering or impose a purely hierarchical structure. Models considering only one grouping factor would overstate the importance of that dimension because variation attributable to the other classification would be absorbed into the remaining variance components (van Landeghem et al., 2005; Moerbeek, 2004; Tranmer and Steel, 2001). Information criteria and likelihood-ratio tests consistently favour the cross-classification specification. The unconditional model therefore provides a

Table 3: Unconditional models for radial increment

	Radial increment			
	Species u_{00j_1}	Ecoreg u_{00j_2}	Both u_{00j_1} and u_{00j_2}	Species heterosk.
b_{000}	-6.2657***	-6.1848***	-6.2491***	-6.2490***
	(0.1531)	(0.1385)	(0.1476)	(0.1476)
NT	10643	10643	10643	10643
LL	-11368.32	-11846.28	-11013.66	-10888.23
AIC	22742.6	23698.6	22035.3	21798.5
BIC	22764.5	23720.4	22064.4	21878.5
VPC/ICC sp (u_{00j_1})	27.47		19.21	19.21
VPC/ICC er (u_{00j_2})		22.06	11.56	11.55
ICC tree			30.77	30.77
VPC res ($\varepsilon_{i(j_1,j_2)t}$)	72.53	77.4	69.23	69.23

Note: *** 1%, ** 5%, * 10% statistical significance. When we allow for heteroskedasticity by species, VPC/ICCs are evaluated by exploiting the "weighted average" of variances.

benchmark against which the contribution of climatic and structural covariates can subsequently be assessed.

In the unconditional models of Table 3, the estimated grand mean, b_{000}, corresponds to a radial increment of approximately 0.19 cm (1.9 mm).

The Variance Partition Coefficients (VPCs), which coincide with Intraclass Correlation Coefficients (ICCs) in unconditional models, quantify the proportion of total variation attributable to each level. They therefore measure the similarity in radial increment among trees belonging to the same cluster and quantify the relative importance of species, ecological regions and individual trees as sources of growth variation.

In the last column of Table 3, the within-group variance differs across species, implying that VPCs are themselves species-specific. We therefore report sample-size-weighted average VPCs. The similarity between the weighted averages and the homoskedastic estimates indicates that species with greater (lower) variance are neither very few nor very numerous (distortion in weights), or that some covariates not yet modelled could interact with the species.

Under heteroskedasticity, the correlation between two randomly selected trees belonging to the same species but possibly different ecological regions (between species, biological differences) is 19.21%. The corresponding correlation for two randomly selected trees located in the same ecological region but belonging to different species (spatial/environmental structuring) is 11.56%. Hence, species account

for almost twice as much unexplained variation as ecological regions, an interesting finding given the equality between the number of species and ecological regions. The combined clustering effect (species plus ecological region) is 30.77%. The remaining 69.23% of the variance reflects within-species-within-region variability at the individual-tree level.

When we compute the fractions of total variance which are attributable to species-level differences, Douglas fir shows the highest specie-level VPC (25%) and ecological-region VPC (15%), indicating relatively low within-species variability or more homogeneity within the specie (59%), whereas Aleppo pine shows the lowest VPC (16% at species level and 9% at ecological region level), indicating high within-species variability (74%).

As we observe multiple trees for at least some combinations of species and ecological regions, we tested for the relevance of the interaction effect, $u_{00j_1} \times u_{00j_2}$ (such that the effect of species will differ for trees from different ecological regions even after accounting for the ecological region main effects). Because the interaction contributes negligible variance, its omission do not bias the remaining cross-classified model parameters (Shi et al., 2010). Instead, in equation (1), we modelled the interaction as fixed shifts to capture group-specific deterministic trends.

The unconditional model establishes that substantial variation exists across both species and ecological regions before climatic and structural covariates are introduced. The conditional models examined next investigate to what extent this variation is explained by climate and whether climate sensitivity itself varies across these two dimensions.

5.1 Conditional models

Tables 4 and 5 report the estimates of the conditional models for radial increment presented and compared in Table 2.

The fixed effect (FE) model cannot estimate the time -invariant $native$ effect; moreover, the effects of $alti$, ss, $gini$ and $p2o5$ are not statistically significant. Since the FE model absorbs species–region heterogeneity, it does not partition variance across species and ecological regions nor allow for heterogeneous climate sensitivity. This restricts inference and may misrepresent uncertainty when cross-level dependence is present (Beretvas, 2011). Also, FE would force the data to be conceptualized as categorical differences, whereas the mixed models offer the distribution of climate sensitivity and BLUPs predictors.

Table 4: Conditional models for radial increment - control variables

	FE	MM	MMR	MMS	MMRS	MMRSD
		u_{00j_1}, u_{00j_2}	u_{00j_1}, u_{00j_2} u_{01j_2}	u_{00j_1}, u_{00j_2} u_{01j_1}	u_{00j_1}, u_{00j_2} u_{01j_1}, u_{01j_2}	Diameter
Tree-level variables, $\mathbf{x}_{i(j_1,j_2)t}$						
ss	0.0987	0.1532***	0.1554***	0.1541***	0.1553***	0.5403***
	(0.0905)	(0.0277)	(0.0277)	(0.0277)	(0.0277)	(0.0294)
$native$	0.0000	-0.4408***	-0.4054***	-0.4317***	-0.3895***	-0.5834***
	(.)	(0.1344)	(0.1295)	(0.1391)	(0.1281)	(0.1331)
Tree-plot-level variables variables, $\mathbf{x}_{ip(j_1,j_2)t}$						
$wolftree$	-0.1250*	-0.1387***	-0.1378***	-0.1366***	-0.1380***	-0.2579***
	(0.0673)	(0.0446)	(0.0446)	(0.0446)	(0.0446)	(0.0433)
Forest stand variables, $\mathbf{x}_{p(j_1,j_2)t}$						
$alti$	0.0002	0.0002***	0.0002***	0.0002***	0.0002***	0.0002***
	(0.0001)	(0.0000)	(0.0000)	(0.0000)	(0.0000)	(0.0000)
$gini$	-0.1729	-0.2430***	-0.2431***	-0.2370***	-0.2434***	-0.8994***
	(0.1537)	(0.0754)	(0.0754)	(0.0754)	(0.0754)	(0.0755)
rdi	-0.4432***	-0.4425***	-0.4432***	-0.4441***	-0.4433***	-0.2645***
	(0.0574)	(0.0209)	(0.0209)	(0.0209)	(0.0209)	(0.0208)
$wfcC$	0.0004*	0.0004*	0.0004*	0.0004*	0.0004*	0.0002
	(0.0002)	(0.0002)	(0.0002)	(0.0002)	(0.0002)	(0.0002)
$wfcC \times tlogC$	-0.0144**	-0.0127***	-0.0133***	-0.0134***	-0.0133***	-0.0138***
	(0.0060)	(0.0037)	(0.0037)	(0.0037)	(0.0037)	(0.0036)
cn_ratio	-0.0178***	-0.0170***	-0.0169***	-0.0169***	-0.0169***	-0.0195***
	(0.0030)	(0.0023)	(0.0024)	(0.0023)	(0.0024)	(0.0022)
$base\_cation \times phD0$	-0.0031**	-0.0031***	-0.0031***	-0.0031***	-0.0031***	-0.0041***
	(0.0011)	(0.0005)	(0.0005)	(0.0005)	(0.0005)	(0.0005)
$base\_cation \times phD1$	-0.0037**	-0.0037***	-0.0037***	-0.0036***	-0.0037***	-0.0043***
	(0.0014)	(0.0005)	(0.0005)	(0.0005)	(0.0005)	(0.0005)
$p2o5$	0.0838	0.0793**	0.0722**	0.0757**	0.0723**	0.1247***
	(0.0546)	(0.0309)	(0.0312)	(0.0310)	(0.0312)	(0.0301)
NT	10643	10643	10643	10643	10643	10643
LL	-10537.1	-10465.3	-10459.3	-10461.9	-10459.3	-10010.9
AIC	21104.2	21018.5	21010.6	21015.7	20986.5	20093.7
BIC	21213.2	21338.5	21345.2	21350.2	21233.8	20355.5

Note: *** 1%, ** 5%, * 10% statistical significance. Fixed effects model (FE) uses cluster $j_1 \times j_2$ standard errors.

Table 5: Conditional models for radial increment - climate variables

	FE	MM	MMR	MMS	MMRS	MMRSD
		u_{00j_1}, u_{00j_2}	u_{00j_1}, u_{00j_2} u_{01j_2}	u_{00j_1}, u_{00j_2} u_{01j_1}	u_{00j_1}, u_{00j_2} u_{01j_1}, u_{01j_2}	Diameter
Climatic variables, plot-specific seasonal climate conditions, $\mathbf{x}_{pc(j_1,j_2)t}$						
$tmin\_sprC$	-0.0776	-0.0709***	-0.0595***	-0.0579***	-0.0595***	-0.0392**
	(0.0475)	(0.0166)	(0.0179)	(0.0175)	(0.0179)	(0.0164)
$prec\_sumC \times tmax\_sumC$	0.0004**	0.0003**	0.0003*	0.0003*	0.0003*	0.0002
	(0.0002)	(0.0001)	(0.0002)	(0.0002)	(0.0002)	(0.0002)
$prec\_sprC$	0.0000	-0.0001	-0.0000	0.0000	-0.0000	0.0000
	(0.0005)	(0.0002)	(0.0003)	(0.0003)	(0.0003)	(0.0002)
$prec\_sprC \times tmean\_sprC$	-0.0005**	-0.0003***	-0.0003***	-0.0003**	-0.0004***	-0.0003***
	(0.0002)	(0.0001)	(0.0001)	(0.0001)	(0.0001)	(0.0001)
Climatic variables, plot-specific seasonal climate conditions, $z_{pc(j_1,j_2)t}$						
$tmean\_sprC$	0.1078*	0.0915***	0.0822***	0.0898***	0.0834***	0.0617***
	(0.0519)	(0.0207)	(0.0251)	(0.0291)	(0.0254)	(0.0227)
Tree-level variables, $\mathbf{x}_{i(j_1,j_2)t}$						
dia_W						-0.4929***
						(0.0156)
dia_B						0.4240
						(0.3519)
VPC sp (u_{00j_1}, u_{01j_1})		13.25	18.99	19.90	19.76	13.49
$avg. - 1 \times sd$			17.96	23.57	20.68	9.05
$avg. + 1 \times sd$			19.12	20.49	17.82	18.44
VPC er (u_{00j_2}, u_{01j_2})		7.26	5.86	6.58	5.51	7.03
$avg. - 1 \times sd$			10.97	6.28	9.84	12.07
$avg. + 1 \times sd$			5.20	6.53	5.70	3.26
VPC tree		20.51	24.85	26.49	25.27	20.52
$avg. - 1 \times sd$			28.93	29.85	30.52	21.11
$avg. + 1 \times sd$			24.32	27.02	23.52	21.69
VPC res ($\varepsilon_{i(j_1,j_2)t}$)		79.49	75.15	73.51	74.73	79.48
at -sd			71.07	70.15	69.48	78.89
at + sd			75.68	72.98	76.47	78.31

Note: *** 1%, ** 5%, * 10% statistical significance. Fixed effects model (FE) uses cluster $j_1 \times j_2$ standard errors. Estimates are heteroskedastic by specie, so that VPC/ICCs are evaluated by exploiting the "weighted average" of variances. As ecological region and specie total variances are functions of variance, covariance and values of spring temperatures, we use three evaluation points corresponding to the average temperature (9 °C) and ± one standard deviation (2.55) of spring temperatures.

Compared to Table 3, Table 5 shows that the inclusion of covariates reduces the unexplained heterogeneity across levels. Species-level variance declines from 19.21% to 13.25%, regional variance from 11.55% to 7.26%, and tree-level variance from 30.77% to 20.51%. Allowing random slopes for spring temperatures at both species and ecological-region levels, increases heterogeneity in climate responses, particularly at the species level. Including diameter (MMRSD model) explains a large share of residual heterogeneity and further improves model fit. The within-diameter term is strongly significant, capturing ontogenetic growth decline and indicating that size structure accounts for a major share of growth heterogeneity across species–region combinations.

The estimated spring temperature effect for the average species and ecological region is positive: a 1 °C increase is associated with approximately 8.34% higher radial growth when precipitation is at its mean (226 mm). The corresponding 95% coverage interval ranges from 6.77% to 9.92% across species and from -0.93% to 17.62% across ecological regions, indicating substantially greater spatial than taxonomy variation in climate sensitivity. By contrast, spring precipitation alone is not statistically significant at the mean spring temperature (9 °C). However, the negative interaction between spring temperature and precipitation indicates that the marginal growth benefit of warmer springs declines under wetter conditions. Late spring minimum temperatures reduce growth by 5.95%, consistent with frost damage and delayed cambial reactivation, whereas summer heat-precipitation interactions have comparatively small effects, highlighting the dominant role of the early growing-season conditions.[5]

Introducing diameter as a structural control (last column of Table 5) attenuates the estimated spring temperature effect from 8.34% to 6.17%. This indicates that part of the temperature–growth relationship in simpler models reflects ontogenetic and compositional differences in tree size rather than purely physiological responses to climate. Conditioning on diameter therefore isolate climate sensitivity among trees of comparable size and renders species- and region-level random effects interpretable as genuine variation in climate response rather than sample composition.

Overall, spring climatic conditions emerge as the primary drivers of inter-annual radial growth, whereas summer climatic conditions play a comparatively

[5]Replacing spring climatic conditions with summer climatic conditions deteriorates model performance (log-likelihood and information criteria) and reduces the estimated temperature effect by about three percentage points (see Appendix A.1).

minor role.

Figure 4 illustrates these average climate responses through predictive margins from the MMRSD model, evaluated over mean-centred spring temperature and precipitation. Because predictions are averaged over species and ecological regions, they represent population-average climate responses rather than group-specific trajectories.

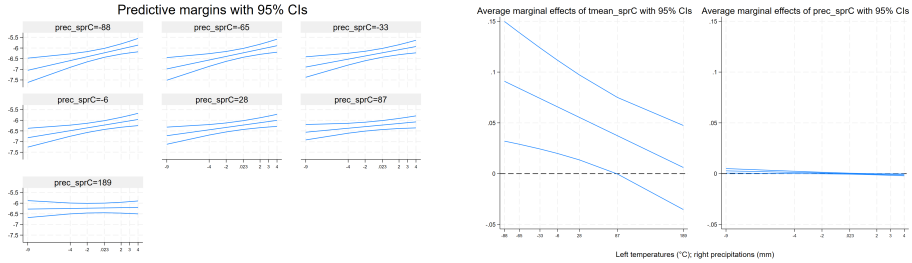

(a) *Predicted radial increment* (b) *Marginal effects*

Figure 4: Spring role on radial increment

The left panel displays predicted radial increment across different spring precipitation regimes. The non-parallel curves provide clear evidence of a negative temperature–precipitation interaction. Under drier-than-average spring conditions, warmer temperatures are associated with a pronounced and statistically significant increase in growth. Around average spring precipitation (approximately 220 mm), the temperature response weakens, whereas under wetter-than-average conditions the marginal effect of temperature becomes progressively attenuated and, at the upper end of the observed precipitation range, is no longer statistically distinguishable from zero. This pattern is confirmed by the corresponding confidence intervals, which intersect zero under the wettest spring conditions.

The right panel of Figure 4 presents the corresponding average marginal effects. The marginal effect of spring temperature declines monotonically with increasing precipitation, whereas the marginal effect of precipitation remains small and statistically weak over the observed temperature range. Thus, spring temperature emerges as the primary climatic driver of radial growth, while spring precipitation primarily modulates the strength of the temperature response rather than exerting an independent influence on growth.

These population-average relationships provide a useful summary of climate effects but conceal substantial variation among species and ecological regions. The following section examines this cross-level heterogeneity through the estimated

random effects and group-specific climate sensitivities.

5.2 Heterogeneous Climate Sensitivity: Species and Regional Random Effects

Figure 5 compare empirical Bayes estimates (BLUPs) of species- and ecological-region-specific random intercepts and spring temperature random slopes under the baseline model (MMRS) and the size-adjusted specification (MMRSD). Each point represents the deviation of a group's intercept (u_{00j}) and spring temperature slope (u_{01j}) from the corresponding population-average fixed effects. Vertical bars denote 95% confidence intervals derived from the estimated random-effect standard errors. Because empirical Bayes estimates are shrinkage estimators, groups with fewer observations are pulled more strongly toward the overall mean and therefore exhibit wider uncertainty intervals. Circle size is proportional to the number of observations within each species or ecological regions.

Species-level responses

Under the baseline specification (MMRS), spring-temperature sensitivity varies substantially among species. Introducing diameter (MMRSD) substantially redistributes the estimated random slopes. Several species change both the magnitude and, in some cases, the sign of their response to spring warming, indicating that part of the apparent interspecific heterogeneity in the baseline model reflects differences in tree size composition rather than intrinsic physiological responses. After accounting for diameter, Aleppo pine (native to Mediterranean) and Silver fir (native to Vosges and Massif Central) exhibit the strongest positive conditional responses to spring warming, whereas European larch (native to Alps) and Scots pine (native to Alps and Massif Central, afforested in Semi-Oceanic Central North) display the weakest responses. Douglas fir, Norway spruce and Maritime pine cluster around the population-average response.

Ecological-region-level responses

Marked differences also emerge across ecological regions. Under the MMRS specification, regions differ substantially in both baseline growth and spring-temperature sensitivity. Introducing diameter (MMRSD) redistributes the estimated regional random slopes, with several regions changing the magnitude and, in some cases, the sign of their temperature response. In particular, the Alps become positively associated with spring warming after accounting for tree size, whereas Oceanic South West and Vosges remain the least responsive regions. environmental differences. These changes indicate that part of the regional heterogeneity observed

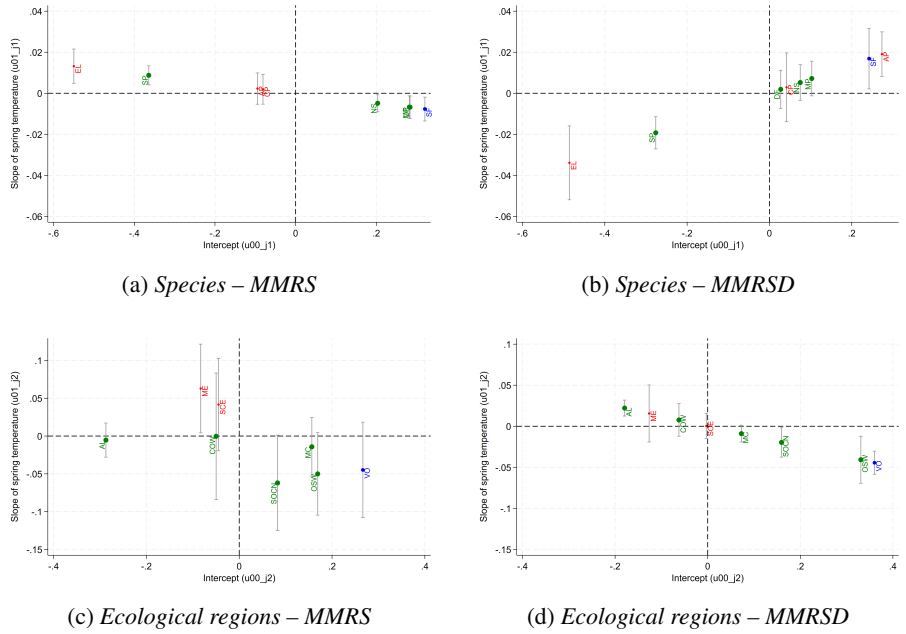

(a) *Species – MMRS* (b) *Species – MMRSD*

(c) *Ecological regions – MMRS* (d) *Ecological regions – MMRSD*

Figure 5: Empirical Bayes estimates of species- and ecological-region-specific random effects.

Note: Points represent empirical Bayes estimates of random intercepts (u_{00j_1} and u_{00j_2}) and random slopes for spring temperature (u_{01j_1} and u_{01j_2}). Vertical bars denote 95% confidence intervals. Circle size reflects the number of observations per species and region (small: < 500; medium: $500 - 999$; large: ≥ 1000). Slopes are deviations from the population-average fixed temperature effect. Species abbreviations: DF = Douglas fir, NS = Norway spruce, EL = European larch, AP = Aleppo pine, CP = Corsican pine, MP = Maritime pine, SP = Scots pine, SF = Silver fir. Ecological region abbreviations: COW = Crystalline and Oceanic West, SOCN = Semi-oceanic Central North, SCE = Semi-continental East, VO = Vosges, OSW = Oceanic South West, MC = Massif Central, AL = Alps, ME = Mediterranean.

in the baseline model is attributable to structural differences in tree size rather than solely to environmental differences.

Overall, comparing MMRS with MMRSD shows that accounting for diameter substantially alters the estimated distribution of climate sensitivity at both the species and ecological-region levels. Although part of the apparent heterogeneity is explained by tree-size composition, considerable variation persists after controlling for ontogenetic effects, confirming that climate sensitivity differs systematically among both species and ecological regions. These remaining differences constitute the basis for the predictive analyses presented in the following section.

5.3 Predicted radial increment

Figure 6 presents locally smoothed predicted radial increment as a function of centred spring mean temperature (Cleveland, 1979). Unlike the marginal effects in Figure 4, these curves represent the realized association between predicted growth and spring temperature across the observed joint distribution of covariates within each species-ecological region combination.[6] Consequently, the trajectories describe conditional growth patterns rather than ceteris paribus temperature effects.

Growth trajectories are obtained from the MMRSD specification. The solid black curve represents the population-average prediction from the fixed component of model (1), $\widehat{y_{Fi(j_1,j_2)t}} = \hat{\beta}_{000} + \mathbf{X}'_{i(j_1,j_2)t}\hat{\boldsymbol{\beta}} + \hat{\theta}_{000}\, z_{pc(j_1,j_2)t}$. The dashed blue curve additionally incorporates species-level random intercepts and slopes, $\widehat{y_{FSi(j_1,j_2)t}} = \widehat{y_{Fi(j_1,j_2)t}} + \hat{u}_{00j_1} + \hat{u}_{01j_1}\, z_{pc(j_1,j_2)t}$, the dashed brown curve adds ecological region-level random effects, $\widehat{y_{FRi(j_1,j_2)t}} = \widehat{y_{Fi(j_1,j_2)t}} + \hat{u}_{00j_2} + \hat{u}_{01j_2}\, z_{pc(j_1,j_2)t}$, whereas the dashed red curve represents the full conditional prediction, $\widehat{y}_{i(j_1,j_2)t} = \widehat{y_{Fi(j_1,j_2)t}} + (\hat{u}_{00j_1} + \hat{u}_{00j_2}) + (\hat{u}_{01j_1} + \hat{u}_{01j_2})\, z_{pc(j_1,j_2)t}$.

This decomposition illustrates how average temperature responses separate into taxonomic and environmental components. Whereas Figure 4 summarises the population-average climate response, Figure 6 reveals that the underlying growth trajectories differ markedly across species-ecological region combinations. In several combinations, spring warming is associated with pronounced increases in predicted growth, whereas in others the response is weak, nearly flat, or even negative.

The decomposition also reveals the origin of this variation. In some combinations, deviations from the population-average trajectory are driven primarily by species-level random effects, while in others ecological context exerts the dominant influence. Consequently, the cross-classified specification separates biological differences among species from contextual differences among ecological regions. Moreover, the MMRSD model demonstrates that part of the apparent variability observed in models without diameter controls reflects differences in size structure rather than intrinsic physiological sensitivity.

Distinct patterns emerge between native and afforested species. Native trees display broadly positive but highly variable responses to spring temperature. Both species identity and ecological context contribute to this variability, and in several

[6] In contrast to Figure 4, covariates are not held fixed at reference values. Predictions follow the empirical joint distribution of precipitations, soil properties, altitude and the remaining explanatory variables within each group.

combinations regional effects modify temperature sensitivity as strongly as, or even more strongly than, species effects. The full conditional prediction therefore emphasize that growth responses arise from the interaction between species traits and environmental setting.

Afforested trees exhibit comparatively more homogeneous trajectories. In many combinations the four predicted curves remain close together, indicating weaker contextual modulation of temperature sensitivity. Species differences are expressed primarily through baseline productivity, whereas temperature responses remain closer to the population-average relationship. Although some introduced species benefit from warmer springs, others display nearly flat trajectories, suggesting that productivity gains under warming are not universal.

Overall, these predicted trajectories reinforce the central result of the paper: spring warming does not produce a uniform response across temperate conifers. Instead, climate sensitivity is jointly determined by species identity, ecological context, and structural characteristics of forest stands. The greater structural and taxonomic diversity typically found in native forests (Felton et al., 2016; Liu et al., 2018) further suggests that differences in conditional growth sensitivity should be interpreted not only in terms of short-term productivity, but also in relation to long-term ecosystem stability and resilience under climate change.

We can note the crossing of the curves. While the intercept shifts the curve vertically, the random slope changes its inclination. A crossing occurs because the relative importance of the intercept and the slope changes with temperature. The crossing of predicted trajectories in some native species–region combinations indicates that the ranking of growth performance changes with spring temperature. Such crossings arise from the joint action of random intercepts and random slopes, implying that climate sensitivity modifies not only the magnitude but also the relative ordering of growth across groups. We observe this mainly for SP-AL. Looking at the numerical BLUPs, the most plausible explanation is that Scots pine in the Alps combines a negative random intercept (low baseline growth) and a positive random slope (high temperature responsiveness). That creates an intersection between the species effect and the ecological-region effect. By contrast, the predominantly parallel trajectories of afforested species indicate that differences are driven mainly by baseline productivity rather than by heterogeneous temperature sensitivity.

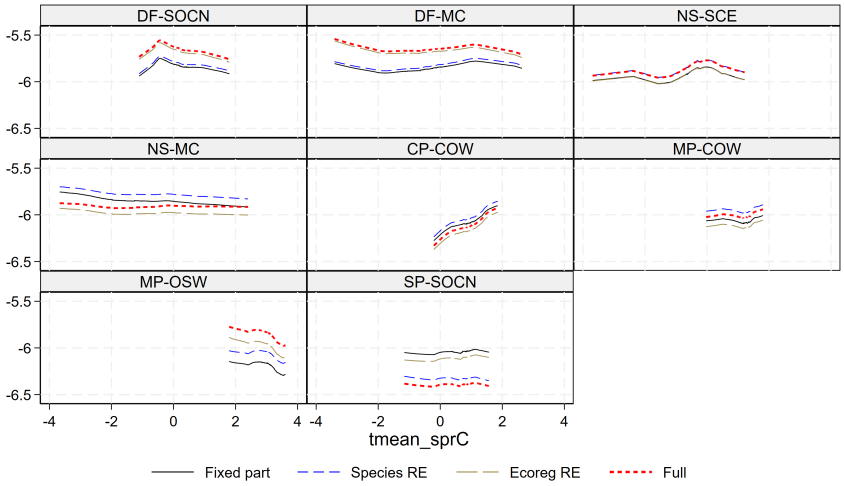

(a) *Afforested trees*

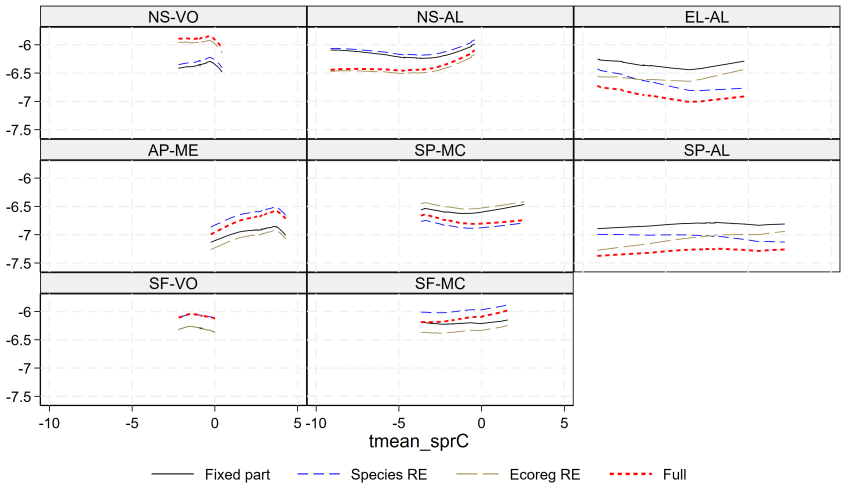

(b) *Native trees*

Figure 6: Predicted growth trajectories

Note: Species abbreviations: DF = Douglas fir, NS = Norway spruce, EL = European larch, AP = Aleppo pine, CP = Corsican pine, MP = Maritime pine, SP = Scots pine, SF = Silver fir. Ecological region abbreviations: COW = Crystalline and Oceanic West, SOCN = Semi-oceanic Central North, SCE = Semi-continental East, VO = Vosges, OSW = Oceanic South West, MC = Massif Central, AL = Alps, ME = Mediterranean.

5.4 Discussion

Results from unconditional models in Table 3 have implications for dendrochronological cross-dating, suggesting that most inter-annual variability in radial growth

occurs at the individual-trees level and that common growth signals may extend across species sharing the same environmental conditions.

In the conditional models reported in Tables 4 and 5, native species grow more slowly even after controlling for site, climate, competition, and tree size. The increase in magnitude of the $native$ coefficient after accounting for diameter suggests that native and introduced stands differ systematically in size structure. This pattern may reflect long-term adaptive strategies. One possible interpretation is that the native species included in our sample adopt more conservative resource-use strategies, prioritising persistence under variable environmental conditions over maximizing short-term growth. Such conservative strategies have been associated with greater tolerance of environmentally stressful conditions through more cautious allocation of carbon, water and nutrients. This interpretation is compatible with the functional framework proposed by Augusto, Borelle, et al. (2025), in which conservative tree species maintain more stable realized growth under environmentally stressful conditions than acquisitive species, although our analyses do not directly classify species according to functional traits or establish that native species are inherently more conservative.

Larger, dominant trees capture a disproportionate share of resources (light, water, and nutrients) and use them more efficiently, reinforcing their competitive advantage, while subordinate individuals exhibit reduced growth (Canham et al., 2004; Binkley, 2004; Binkley et al., 2010). Controlling for size structure amplifies the estimated dominance effect, suggesting that social status captures competitive asymmetry beyond ontogenetic size effects, that is, the tendency for larger trees to exhibit lower radial increment. High stand density further intensifies crowding and suppresses smaller individuals (Zhang et al., 2018; Chi et al., 2015; Linger and Long, 2025). Moderate heterogeneity may sustain diversity and resilience, whereas pronounced heterogeneity can reduce stand-level efficiency by limiting the contribution of subordinate individuals (Binkley et al., 2010). The MMRSD specification suggests that diameter absorbs part of the structural heterogeneity and that density effects partly operate through size structure.

Importantly, site-specific conditions, particularly soil texture and depth determining water capacity, can modulate negative climate impacts (Lundgren et al., 2025; Anderson-Teixeira et al., 2022), influencing both water accessibility during the growing season and sensitivity to precipitation variability and drought (Leuschner, 2020; van der Maaten-Theunissen et al., 2013).

Tree social status may further influence drought responses, although the direc-

tion of this effect remains debated. Dominant trees benefit from greater resource acquisition under favourable conditions, but their larger crowns and higher transpiration demands may increase vulnerability during severe droughts. Conversely, suppressed trees experience chronic resource limitation, which may reduce their capacity to withstand prolonged water deficits. Our results suggest that stand structure and competitive interactions should therefore be considered jointly when evaluating climate sensitivity. Shallow or coarse-textured soils restrict rooting depth and water storage, whereas deeper soils provide larger reserves that sustain productivity. Soil pH and nutrient availability also play a central role, as acidity and nutrient imbalances can limit resource uptake and reduce growth efficiency (Augusto and Boča, 2022; Jonard et al., 2015).

Elevation regulates temperature regimes and the length of the growing season. Warming has already driven many tree species to establish and regenerate at higher altitudes, effectively shifting their distributions upslope across Europe (Lenoir et al., 2008). Lowland stands tend to be water-limited, whereas high-elevation stands are more constrained by shorter, cooler growing seasons, highlighting elevation as a fundamental control of forest dynamics (van der Maaten-Theunissen et al., 2013).

Our finding that spring climatic conditions are the primary drivers of interannual radial growth is biologically plausible because earlywood constitutes the largest fraction of annual ring formation and is produced during the period of most intense cambial activity. Consequently, climatic conditions during spring exert a stronger influence on annual radial increment than those prevailing later in the growing season. By contrast, analyses focusing on wood density would likely attribute greater importance to summer climatic conditions because latewood formation occurs during that period.

More broadly, our results illustrate the importance of jointly modelling biological and environmental sources of heterogeneity. By accounting simultaneously for cross-classified species and ecological-region effects, together with tree-size structure, the proposed framework separates structural differences in growth from genuine differences in climate sensitivity. This distinction is essential for identifying which components of forest vulnerability arise from species composition, environmental context, or stand structure under climate change.

6 Conclusions

Climate sensitivity in temperate conifer forests cannot be adequately represented by a single average response. By combining a national-scale forest inventory with a cross-classified mixed modelling framework, we disentangle the joint contributions of species identity, ecological context and stand structure to inter-annual radial growth, providing a more comprehensive assessment of forest responses to climate change.

Our results identify spring climatic conditions as the dominant driver of radial growth, while demonstrating that both the magnitude and, in some cases, the direction of temperature responses vary substantially across species and ecological regions. Accounting for tree size through within- and between-tree diameter decomposition reveals that part of the apparent heterogeneity reflects structural differences in stand composition rather than intrinsic physiological responses to climate. Nevertheless, considerable variation persists after controlling for ontogenetic effects, confirming that climate sensitivity is jointly determined by biological and environmental factors.

Beyond these methodological contributions, our findings suggest contrasting ecological strategies between native and introduced species. Native species grow more slowly even after controlling for climate, site conditions, competition and tree size, whereas introduced species generally exhibit higher growth potential. One possible interpretation is that the native species considered in our study adopt more conservative resource-use strategies, prioritising persistence under variable environmental conditions over maximizing short-term growth. Although this hypothesis requires direct physiological validation, it provides a promising avenue for future research into the adaptive strategies of temperate forests under climate change.

More broadly, our findings support the argument of Holtmeier and Broll (2005) that biological responses to global environmental change cannot be understood from climate alone, but must be interpreted across interacting biological, environmental and temporal scales. By jointly modelling species identity, ecological context and stand structure, our framework shows that climate sensitivity is intrinsically structured rather than homogeneous. Consequently, forest responses to continued warming are unlikely to occur as uniform shifts, but rather as spatially differentiated adjustments in which species track locally favourable climatic and edaphic conditions (Lenoir et al., 2008).

These findings have important implications for both ecological forecasting and forest management. Dynamic projections based on species- or region-aggregated responses risk masking substantial differences in climate sensitivity and may therefore produce misleading estimates of future forest productivity. Reliable projections require explicit consideration of cross-level heterogeneity, stand structure and ecological context. Likewise, management strategies that promote structurally diverse stands and species adapted to local environmental conditions are likely to enhance resilience under continued climate change.

Ultimately, forest adaptation to climate change should be viewed as a problem of differential sensitivity rather than average response. Climate sensitivity is a structured, multilevel property of forest ecosystems, emerging from the interaction between species traits, ecological context and stand structure. Recognising this cross-level heterogeneity is essential for understanding, predicting and managing forest dynamics in a rapidly changing climate.

Acknowledgements

We are grateful to the participants at the 30th and 31st Annual International Panel Data Conferences (University of Montpellier and University of Exeter) and at the 5th Italian Workshop of Econometrics and Empirical Economics (Università Politecnica delle Marche, Ancona) for their valuable comments and suggestions.

We are particularly grateful to Matilde Bontempo for carefully checking parts of the manuscript, and to Alessandro Liverani for his insightful comments and for generously sharing his expertise in forestry.

Finally, we owe our deepest gratitude to Jacques Mairesse for bringing the two authors together. Without him, this collaboration—and therefore this paper—would never have happened.

References

Aakala, T., S. Fraver, A. W. D'amato, and B. J. Palik (2013). "Influence of competition and age on tree growth in structurally complex old-growth forests in northern Minnesota, USA". In: *Forest Ecology and Management* 308, pp. 128–135.

Allen, C. D. et al. (2010). “A global overview of drought and heat-induced tree mortality reveals emerging climate change risks for forests”. In: *Forest Ecology and Management* 259, pp. 660–684.

Anderson-Teixeira, K. J., V. Herrmann, C. R. Rollinson, B. Gonzalez, E. B. Gonzalez-Akre, N. Pederson, M. R. Alexander, C. D. Allen, and et al. (2022). “Joint effects of climate, tree size, and year on annual tree growth derived from tree-ring records of ten globally distributed forests”. In: *Global Change Biology* 28, pp. 245–266.

Augusto, L. and A. Boča (2022). “Tree functional traits, forest biomass, and tree species diversity interact with site properties to drive forest soil carbon”. In: *Nature Communications* 13.1, p. 1097. DOI: 10.1038/s41467-022-28748-0.

Augusto, L., R. Borelle, et al. (2025). “Widespread slow growth of acquisitive tree species”. In: *Nature* 640, pp. 395–401.

Augusto, L., A. De Schrijver, L. Vesterdal, A. Smolander, C. Prescott, and J. Ranger (2015). “Influences of evergreen gymnosperm and deciduous angiosperm tree species on the functioning of temperate and boreal forests”. In: *Biological Reviews of the Cambridge Philosophical Society* 90:2, pp. 446–466.

Bauhus, J., D. I. Forrester, H. Pretzsch, A. Felton, P. Pyttel, and A. Benneter (2017). *Mixed-species forests: the development of a forest management paradigm*. Ed. by H. Pretzsch, D. I. Forrester, and J. Bauhus. Springer Berlin Heidelberg, pp. 1–25.

Bauman, D. et al. (2022). “Tropical tree growth sensitivity to climate is driven by species intrinsic growth rate and leaf traits”. In: *Global change biology* 28:4, pp. 1414–1432.

Beretvas, S. N. (2011). “Cross-classified and multiple membership models”. In: *Handbook of Advanced Multilevel Analysis*. Ed. by J. J. Hox and J. K. Roberts. Routledge, Taylor & Francis Group, New York and Hove.

Binkley, D. (2004). “A hypothesis about the interaction of tree dominance and stand production through stand development”. In: *Forest Ecology and Management* 2-3, pp. 265–271. DOI: 10.1016/j.foreco.2003.10.018.

Binkley, D., J. L. Stape, W. L. Bauerle, and M. G. Ryan (2010). “Explaining growth of individual trees: light interception and efficiency of light use by Eucalyptus at four sites in Brazil”. In: *Forest Ecology and Management* 259 (9), pp. 1704–1713.

Bouvet, A., N. Nguyen-The, and F. Melun (2013). "Nutrient concentration and allometric models for hybrid eucalyptus planted in France". In: *Annals of Forest Science* 70, pp. 251–260.

Brang, P. et al. (2014). "Suitability of close-to-nature silviculture for adapting temperate European forests to climate change". In: *Forestry: An International Journal of Forest Research* 87.4, pp. 492–503.

Bremer, L. L. and K. A. Farley (2010). "Does plantation forestry restore biodiversity or create green deserts? A synthesis of the effects of land-use transitions on plant species richness". In: *Biodiversity and Conservation* 19, pp. 3893–3915.

Bruijnzeel, L. A. (2004). "Hydrological functions of tropical forests: not seeing the soil for the trees?" In: *Agriculture, Ecosystems & Environment* 104, pp. 185–228.

Canham, C., P. LePage, and K. Coates (Apr. 2004). "A neighborhood analysis of canopy tree competition: effects of shading versus crowding". In: *Canadian Journal of Forest Research-Revue Canadienne De Recherche Forestiere* 34, pp. 778–787. DOI: 10.1139/x03-232.

Chi, X., Z. Tang, Z. Xie, Q. Guo, M. Zhang, J. Ge, G. Xiong, and J. Fang (2015). "Effects of size, neighbors, and site condition on tree growth in a subtropical evergreen and deciduous broad-leaved mixed forest in China". In: *Ecology and Evolution* 5(22), pp. 5149–5161.

Cleveland, W. S. (1979). "Robust locally weighted regression and smoothing scatterplots". In: *Journal of the American Statistical Association* 74, pp. 829–836.

Collado, E., J. J. Camarero, J. Martínez de Aragón, J. Pemán, J. A. Bonet, and S. de-Miguel (2018). "Linking fungal dynamics, tree growth and forest management in a Mediterranean pine ecosystem". In: *Forest Ecology and Management* 422, pp. 223–232.

Cornes, R. C., G. van der Schrier, E. J. M. van den Besselaar, and P. D. Jones (2018). "An ensemble version of the E-OBS temperature and precipitation datasets". In: *Journal of Geophysical Research: Atmospheres* 123.17, pp. 9391–9409. DOI: 10.1029/2017JD028200.

European Environment Agency (2020). *Climate change impacts in Europe*. EEA Report.

Evans, M. E. K., D. A. Falk, A. Arizpe, T. L. Swetnam, F. Babst, and K. E. Holsinger (2017). "Fusing tree-ring and forest inventory data to infer influences on tree growth". In: *Ecosphere* 8(7), e01889.

Felton, A., U. Nilsson, J. Sonesson, and et al. (2016). "Replacing monocultures with mixed-species stands: Ecosystem service implications of two production forest alternatives in Sweden". In: *Ambio* 45 (Suppl 2), pp. 124–139.

Gentilesca, T. and L. Todaro (2008). "Crescita radiale e risposte climatiche dell'abete bianco (Abies alba Mill.) in Basilicata". In: *Forest@* 5, pp. 47–56. URL: http://www.sisef.it/forest@/.

Goldstein, H. (2011). *Multilevel Statistical Models*. John Wiley & Sons, Ltd, 4th Ed.

Gong, S., S. Liu, F. Li, G. Xu, J. Chen, L. Jia, and Z. Shi (2025). "Natural forests vs. plantations: A meta-analysis of consequences for soil organic carbon functional fractions". In: *Journal of Environmental Management* 377, p. 124673.

Gortan, M., L. Testa, G. Fagiolo, and F. Lamperti (2024). "A unified dataset for pre-processed climate indicators weighted by gridden economic activity". In: *Scientific Data* 11:1, p. 533.

Gschwantner, T., A. Lanz, C. Vidal, M. Bosela, L. Di Cosmo, J. Fridman, P. Gasparini, A. Kuliešis, S. Tomter, and K. Schadauer (2016). "Comparison of methods used in European National Forest Inventories for the estimation of volume increment towards harmonisation". In: *Annals of Forest Science* 73, pp. 807–821.

Hanewinkel, M., D. A. Cullmann, M.-J. Schelhaas, G.-J. Nabuurs, and N. E. Zimmermann (2013). "Climate change may cause severe loss in the economic value of European forest land". In: *Nature Climate Change* 3, pp. 203–207.

Hlásny, T., P. Krokene, A. Liebhold, C. Montagné-Huck, J. Müller, H. Qin, K. Raffa, M.-J. Schelhaas, R. Seidl, M. Svoboda, et al. (2019). *Living with bark beetles: impacts, outlook and management options*. Vol. 8. EFI Joensuu.

Holtmeier, F. K. and G. Broll (2005). "Sensitivity and response of northern hemisphere altitudinal and polar treelines to environmental changes at landscape and local scale". In: *Global ecology and Biogeography* 14, pp. 395–410.

Intergovernmental Panel on Climate Change (2022). *Climate Change 2022: Impacts, Adaptation and Vulnerability*. Sixth Assessment Report.

Jonard, M. et al. (2015). "Tree mineral nutrition is deteriorating in Europe". In: *Global Change Biology* 21, pp. 418–430.

Kitikidou, K. and E. Apostolopoulou (2011). "Applying survival analysis for assessment of forests sustainable development". In: *Renewable and Sustainable Energy Reviews* 15.1, pp. 851–855. DOI: 10.1016/j.rser.2010.08.008.

Klesse, S. et al. (2020). "Continental-scale tree-ring based projection of Douglas-fir growth: Testing the limits of space-for-time substitution". In: *Global Change Biology* 26.9, pp. 5146–5163. DOI: 10.1111/gcb.15241.

Lenoir, J., J.-C. Gégout, P. A. marquet, and P. de Ruffray (2008). "A significant upward shift in Plant species optimum elevation during the 20th century". In: *Science* 320(5884), pp. 1768–1771.

Leuschner, C. (2020). "Water relations and forest productivity". In: *Annals of Forest Science* 77, p. 69.

Lindner, M. et al. (2010). "Climate change impacts, adaptive capacity, and vulnerability of European forest ecosystems". In: *Forest Ecology and Management* 259, pp. 698–709.

Linger, E. and W. Long (2025). "Phosphorus limitation constrains global forest productivity directly and indirectly via forest commnunity structural attributes: meta-analsysi". In: *Global Ecology and Biogeography* 34:5, e70048.

Liu, C. L. C., O. Kuchma, and V. Krutovsky (2018). "Mixed-species versus monocultures in plantation forestry: development, benefits, ecosystem services and perspectives for the futire". In: *Global Ecology and Conservation* 15, e00419.

Lundgren, A., J. Strengbom, J. Edvardsson, and G. Granath (2025). "Unpacking climate effects on boreal tree growth: An analysis of tree-ring widths across temperature and soil moisture gradients". In: *EGUsphere* 2361, pp. 1–27. DOI: 10.5194/egusphere-2025-2361.

Magarik, Y., L. Roman, and J. Henning (Nov. 2019). "How should we measure the DBH of multi-stemmed urban trees?" In: *Urban Forestry & Urban Greening* 47, p. 126481. DOI: 10.1016/j.ufug.2019.126481.

Mencuccini, M., J. Martínez-Vilalta, D. Vanderklein, H. A. Hamid, E. Korakaki, S. Lee, and B. Michiels (2005). "Size-mediated ageing reduces vigour in trees". In: *Ecology Letters* 8.11, pp. 1183–1190. DOI: 10.1111/j.1461-0248.2005.00819.x.

Moerbeek, M. (2004). "The Consequence of Ignoring a Level of Nesting in Multilevel Analysis". In: *Multivariate Behavioral Research* 39.1, pp. 129–149.

Mohr, J., D. Thom, H. Hasenauer, and R. Seidl (2024). "Are uneven-aged forests in Central Europe less affected by natural disturbances than even-aged firests?" In: *Forest Ecology and Management* 559, p. 121816.

Mundlak, Y. (1978). "On the pooling of time series and cross-sectional data". In: *Econometrica* 46, pp. 69–86.

Nabuurs, G.-J. (2018). “Future scenarios of European forests”. In: *Journal of lanss-cape Ecology* 11(3), pp. 175–184.

Ols, C., T. Gschwantner, K. Schadauer, and J.-D. Bontemps (2022). “Unexpected Negative Effect of Available Water Capacity Detected on Recent Conifer Forest Growth Trends Across Wide Environmental Gradients”. In: *Ecosystem* 25, pp. 404–421.

Ols, C., J.-C. Hervé, and J.-D. Bontemps (2020). “Recent growth trends of conifers across Western Europe are controlled by thermal and water constraints and favored by forest heterogeneity”. In: *Science of the Total Environment* 742, 140453.

Pan, Y., R. a. Birdsey, J. fang, and R. A. Houghton (2011). “A large and persistent carbon sink in the world’s forests”. In: *Science* 333, pp. 988–993.

Pretzsch, H., P. Biber, G. Schütze, E. Uhl, and T. Rötzer (2014). “Forest stand growth dynamics in Central Europe have accelerated since 1870”. In: *Nature Communications* 5, p. 4967.

Rasbash, J. and W. J. Browne (2001). “Modelling non-hierarchical structures”. In: *Multilevel Modelling of Health Statistics*. Ed. by A. H. Leyland and H. Goldstein. Chichester: Wiley.

Rasbash, J. and W. J. Browne (2008). “Non-hierarchical multilevel models”. In: *Handbook of Multilevel Analysis*. Ed. by D. J. and M. E. New York: Springer.

Rasbash, J. and H. Goldstein (1994). “Efficient analysis of mixed hierarchical and cross-classified random structures using a multilevel model”. In: *Journal of Educational and Behavioral Statistics* 19, pp. 337–350.

Ryan, M. G. and B. J. Yoder (1997). “Hydraulic limits to tree height and tree growth”. In: *Bioscience* 47.4, pp. 235–242.

Sheikh, M. A., A. Tiwari, J. Anjum, and S. Sharma (2021). “Dynamics of carbon storage and status of standing vegetation in temperature coniferous forest ecosystem of north western Himalaya India”. In: *Vegetos* 34:4, pp. 822–833.

Shi, Y., W. Leite, and J. Algina (2010). “The impact of omitting the interaction between crossed factors in cross-classified random effect modelling”. In: *British Journal of Mathematica and Statistical Psychology* 63, pp. 1–15.

Tranmer, M. and D. G. Steel (2001). “Ignoring a level in a multilevel model: Evidence from UK census data”. In: *Environment and Planning A: Economy and space* 33, pp. 941–948.

Tsunetsugu, Y., B. J. Park, and Y. Miyazaki (2009). “Trends in research related to “Shinrin-yoku” (taking in the forest atmosphere or forest bathing) in Japan”. In: *Environmental Health and Preventive Medicine* 15, pp. 27–37.

van der Maaten-Theunissen, M., H. P. Kahle, and E. van der Maaten (2013). “Drought sensitivity of Norway spruce is higher than that of Silver fir along an altitudinal gradiente in suothwestern Germany”. In: *Annals of Forest Science* 70:2, pp. 185–193.

van Landeghem, G., B. De Fraine, and J. van Damme (2005). “The Consequence of Ignoring a Level of Nesting in Multilevel Analysis: A Comment”. In: *Multivariate Behavioral Research* 40.4, pp. 423–434.

Waring, B., M. Neumann, I. Colin Prentice, M. Adams, P. Smith, and M. Siegert (2020). “Forests and Decarbonization – Roles of Natural and Planted Forests”. In: *Frontiers in Forests and Global Change* 3.

Zhang, J., D. Guan, W. Li, D. Sun, C. Jin, Y. F., A. Wang, and J. Wu (2018). “The effects of forest thinning on soil carbon stocks and dynamics: A mete analysis”. In: *Forest Ecology and Management* 429, pp. 36–43.

A.1 Appendix

A.1.1 Theoretical heterogeneity in the data

An idea of the heterogeneity in growth patterns and life-span characteristics in the dataset, is from Table A.1, reporting, for each species, the "theoretical" range of radial increment and diameter, and a brief description of the main silvicultural traits.

Table A.1: "Theoretical" Conifer Species characteristics

Species, common (scientific) name	Radial Increment range (cm/year)	Diameter range (m)	Notes and average lifespan
Douglas fir (*Pseudotsuga menziesii*)	0.3–0.77	0.6–1.2	High growth potential on productive sites, 700y.
Maritime pine (*Pinus pinaster*)	0.2–0.4	0.4–0.8	Common in coastal and Atlantic regions, 100-200y.
Norway spruce (*Picea abies*)	0.2–5	0.4–0.8	Sensitive to drought; good on moist soils, 200-300y.
Corsican pine (*Pinus nigra subsp. laricio*)	0.15–0.4	0.5–0.9	Performs well in Mediterranean uplands, 100-200y.
Silver fir (*Abies alba*)	0.2–0.5	0.6–1.0	Sensitive to late frost and early drought, 200-400y.
Aleppo pine (*Pinus halepensis*)	0.1–0.3	0.3–0.6	Drought-tolerant; low growth in dry sites, 100-150y.
Scots pine (*Pinus sylvestris*)	0.1..0.4	0.3–0.7	Widespread; variable depending on site, 150-300y.
European larch (*Larix decidua*)	0.2–0.5	0.4–0.8	Deciduous; fast early growth, 250-500y.

A.1.2 Spatial and Temporal Patterns of Climate

Climate conditions vary widely across French ecological regions, reflecting the marked environmental heterogeneity of the country and making it a privileged setting for analysing tree growth under diverse regimes. Table A.2 reports mean seasonal temperature and precipitation (together with their standard deviations) by ecological region, highlighting the spatial variability in climate across the French territory. Distinct climatic patterns emerge, from the warm and dry Mediterranean south to the cold and humid alpine zones, while intermediate oceanic and continental regions exhibit more moderate conditions.

Besides the spatial climatic variation that is captured at the plot level, climate also shows that the combination of warming and increase in precipitation has become a concern, raising questions about the long-term resilience of forests to climatic extremes. Alps are characterised by extremely cold temperatures and high precipitations in 2011-2013, and Vosges by positive outliers in precipitations of 2006 and 2011. Overall, seasonal temperatures across plots have increased in 2008-2009 and in 2014-2016; seasonal precipitations show the occurrence of anomalous years with droughts or altered rainfall patterns, which represent critical stress factors for conifers, in 2007, 2009, 2016, while 2008, 2011, 2015-2016 are characterised by increased rainfalls.

The dashboard of spatially weighted climate variables from Gortan et al. (2024) is useful for examining annual climate anomalies, as it provides weighted averages

that take into account socio-economic distributions (e.g., population, night lights, cropland) when aggregating grid data to administrative units such as countries, so that the values reflect the actual location of people and economic activity. For France, the years 2011 and 2014 are confirmed to be particularly warm (above 12.6 °C), while 2009, 2013 and 2014 were characterised by high precipitations (above 850 mm).

Table A.2: Mean seasonal temperature (°C) and precipitations (mm)

Ecoregion	Spring	Summer	Autumn	Winter
1-Crystalline and Oceanic West	10.49	18.26	12.11	5.18
	(0.41)	(0.69)	(0.49)	(0.79)
	170.9	137.6	196.2	205.5
	(13.80)	(14.65)	(26.51)	(34.20)
2-Semi-Oceanic Central North	9.93	17.92	11.31	4.04
	(0.51)	(0.74)	(0.64)	(1.06)
	182.8	163.6	203.7	201.5
	(20.01)	(25.66)	(29.25)	(35.42)
3-Semi-Continental East	8.93	17.19	9.93	2.18
	(0.74)	(0.91)	(0.60)	(0.57)
	217.0	213.2	242.1	254.7
	(28.35)	(24.91)	(35.86)	(40.15)
4-Vosges	8.37	16.85	9.28	1.25
	(0.63)	(0.60)	(0.43)	(0.42)
	286.2	272.5	320.7	359.8
	(44.99)	(32.66)	(52.26)	79.92)
5-Oceanic South West	12.42	20.06	14.28	7.22
	(0.37)	(0.20)	(0.56)	(0.72)
	224.6	166.5	262.5	257.9
	(32.50)	(22.43)	(39.61)	(34.69)
6-Massif Central	8.04	16.79	9.88	2.35
	(1.27)	(1.19)	(1.11)	(1.12)
	241.2	199.6	275.6	215.7
	(29.38)	(20.27)	(47.79)	(45.49)
7-Alps	5.91	15.28	8.13	0.37
	(2.78)	(2.75)	(2.59)	(2.20)
	267.5	182.1	341.9	274.1
	(54.69)	(52.45)	(40.96)	(56.26)
8-Mediterranean	12.33	21.61	14.38	6.63
	(0.82)	(0.81)	(0.80)	(0.88)
	160.4	90.2	245.2	169.7
	(16.01)	(15.07)	(31.59)	(19.18)
Total	9.41	17.81	11-16	3.74
	(2.55)	(2.26)	(2.49)	(2.72)
	226.16	179.80	266.30	238.32
	(48.27)	(45.28)	(60.05)	(61.42)

Note: Standard deviations in parentheses.

A set of *year-specific* regressions was estimated to assess whether the relationship between climate and growth changes over time during the period 2006 to 2016,

and for each season (summer, spring, autumn, winter). The specification includes the same controls used in conditional models (*ss, gini, wolf_focal, rdi, wfcC, . . . , altitude, native*, together with seasonal precipitation, temperature, and their interaction. The results are visualised through the coefficient plots in Figures A.1-A.3 from 2006 to 2016, just to confirm that spring seems to be the most relevant for the resumption of the trees' growth cycle.

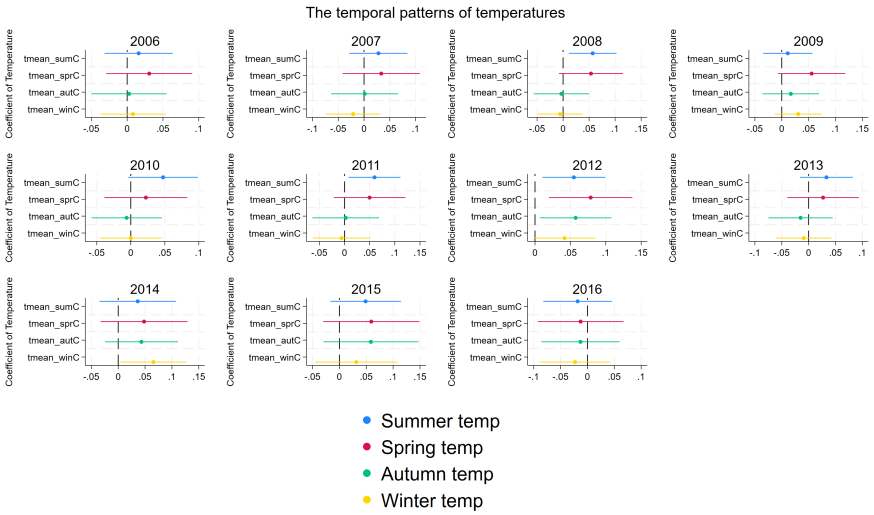

Figure A.1: Coefficient estimates of mean temperature in yearly models, 2006–2016. Horizontal bars indicate 95% confidence intervals.

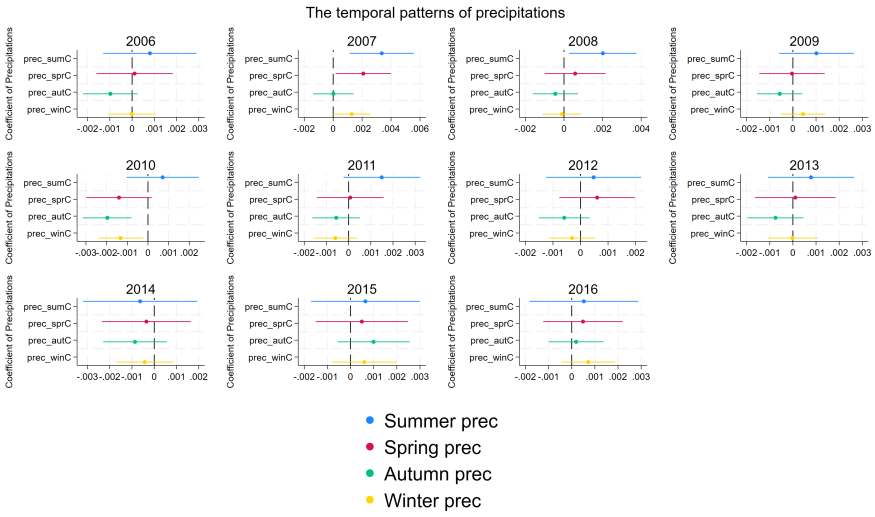

Figure A.2: Coefficient estimates of precipitations in yearly models, 2006–2016. Horizontal bars indicate 95% confidence intervals.

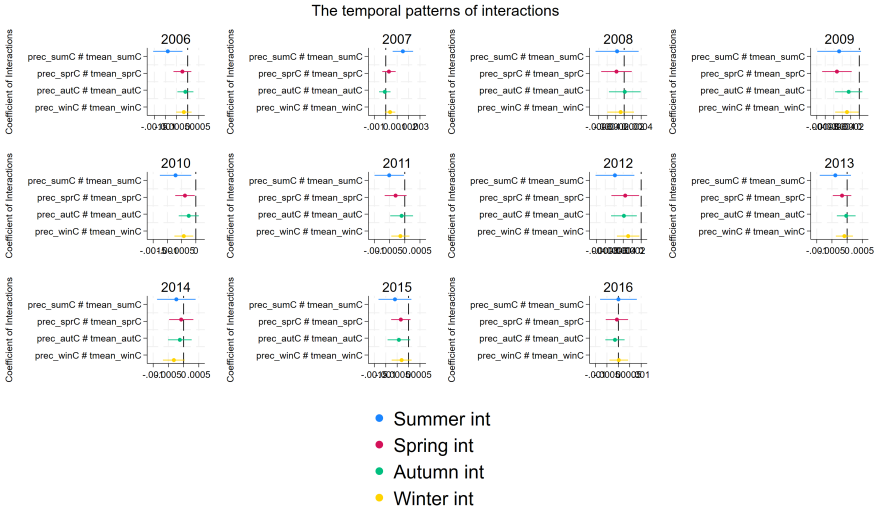

Figure A.3: Coefficient estimates of the interaction between mean temperature and precipitations in yearly models, 2006–2016. Horizontal bars indicate 95% confidence intervals.

Mean temperature tends to be mostly positive and significant in 2008-2009, 2011-2012, and negative in 2016. Parameters –typically around 0.03–0.08–indicate that one °C more in spring temperatures is associated with roughly 5.5% increment in radial growth (similar effects in summer) when precipitations are at their average

(226 mm in spring). Spring precipitation is positive and significant in 2007 and negative in 2010; the average estimated effect is 0.001, meaning an increment in radial growth of 0.1% when temperatures are at the average (9 °C in spring). By contrast, the precipitation × temperature interaction is mainly negative and significant particularly in 2009–2012, indicating that warm and wet seasons depress growth; 2007 is the exception with both temperature, precipitation and their interaction significantly positive. Taken together, these patterns suggest that higher temperatures and precipitation tended to be individually beneficial, but their combination (higher temperatures and heavier rainfalls) tended to be detrimental—consistent with mechanisms such as heat- and moisture-related stress outweighing otherwise favourable moisture or warmth.

A.1.3 Additional checks

Although growing less on average in terms of radial increment, native trees react more positively to rainfall and, in particular, to temperatures, as illustrated in Figure A.4. For example, *native* × *Prec_sprC* is positive (≈ 0.002), implying that natives gain about 0.2% additional growth per extra mm of spring rain. These findings are consistent with the literature, which reports that native species often grow more slowly than many introduced species used in monocultures, as the latter have been specifically selected for rapid growth. At the same time, however, native trees tend to be more stable under climate stress because they are better adapted to their local environments.

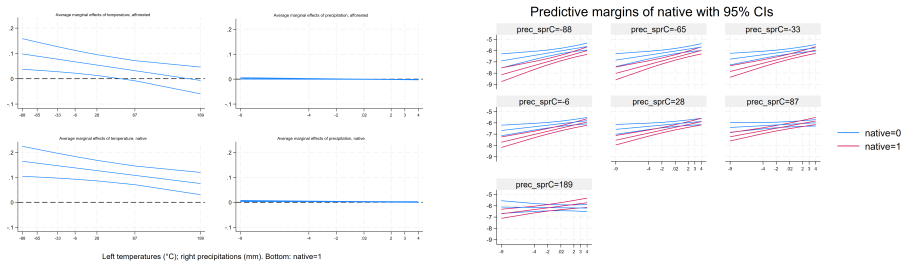

(a) *Spring effects by native* (b) *Predicted growth by spring effects and native*

Figure A.4: Spring effects on radial increment by native

Figure A.5 shows that the Gini index tends to be positive for elevated precipitations, indicating that more heterogeneous stands benefit more from rainfall, and that the dangerousness of elevated temperatures and precipitations is smoothed by

high altitudes.

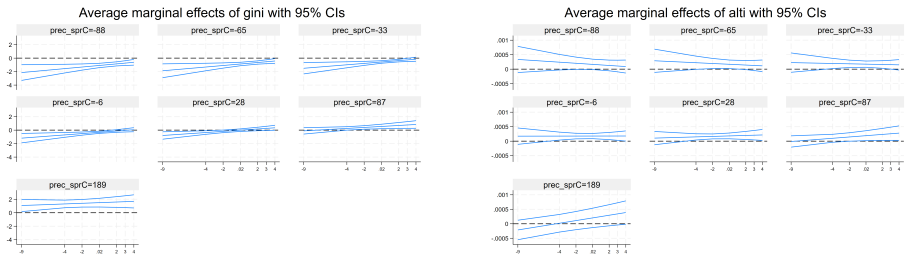

(a) *Spring effects by Gini index* (b) *Spring effects by elevation*

Figure A.5: Focus on Gini index and elevation

Regarding competition, the wolf tree reduces growth in Douglas fir and Norway spruce. Taking Douglas fir (the specie with the highest radial increment) as benchmark, rdi (the tree Relative Density Index) reduces growth in Corsican pine, Aleppo pine, European larch and Maritime pjne; the $gini$ index penalises growth of Corsican pine, while it increases growth of Norway spruce, Maritime pine and European larch. The specie with the highest diameter is Silver fir; the wolf tree reduces diameter growth of Maritime pine and Scots pine, while increases that of European larch; the rdi reduces diameter growth of Scots pine, Silver fir, Norway spruce and Aleppo pine; the $gini$ index on diameter penalises Silver fir, while stimulates Corsican pine.

The quantile-quantile plots of random effects and residuals, in Figure A.6, confirm that European Larch in Alps is a negative outlier at the species-level and Norway spruce in Vosges and Maritime pine in Oceanic south west are negative outliers at the regional level.

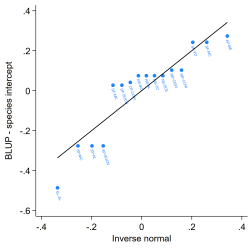

(a) *Predicted intercepts at species level*

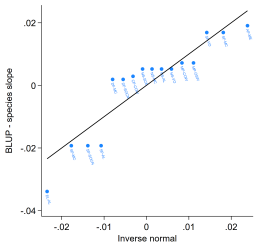

(b) *Predicted slopes at species level*

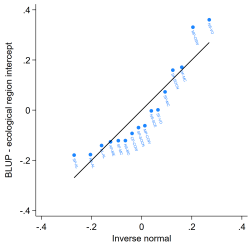

(c) *Predicted intercepts at region level*

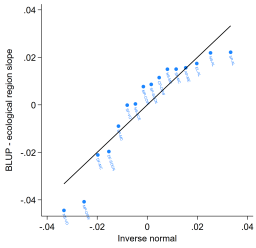

(d) *Predicted slopes at region level*

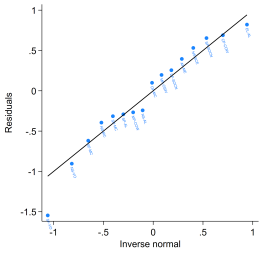

(e) *Residuals*

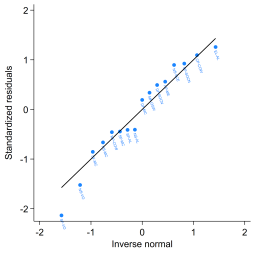

(f) *Standardized residuals*

Figure A.6: Predicted random effects and residuals from MMRSD model

Alma Mater Studiorum - Università di Bologna

DEPARTMENT OF ECONOMICS

Strada Maggiore 45
40125 Bologna - Italy
Tel. +39 051 2092604
Fax +39 051 2092664
http://www.dse.unibo.it